Project	ICESTARS
Project Number	FP7/2008/ICT/214911
Work Package	WP3
Tasks	T3.2 and T3.3
Deliverable	D3.2 - version 1.0

title	Report on the implementation of the RF boundary conditions and the transient simulation with adaptive computing facilities
authors	Wim Schoenmaker, Peter Meuris Monica Selva Soto Sascha Baumanns, Michael Matthes Caren Tischendorf, Thorsten Sickenberger
Affliations	MAGWEL University of Cologne
date	October 2, 2009

ICESTARS FP7/2008/ICT/214911 D3.2

Report on the implementation of the RF boundary conditions and the transient simulation with adaptive computing facilities

Wim Schoenmaker, Peter Meuris
(MAGWEL)

Monica Selva Soto
Sascha Baumanns, Michael Matthes
Caren Tischendorf, Thorsten Sickenberger *
(University of Cologne)

October 2, 2009

Contents

*early stage contribution

1 Introduction

This document describes the mathematical approach that is selected for the activities in WP3 of ICESTARS. In order to support compact model building, we need ab-initio field solving to verify / falsify approximations that are made, while building the compact models. Whereas in the frequency domain, a compact modeling procedure was developed in the projects CODESTAR and CHAMELEON-RF, such a procedure was not yet successfully implemented in the time domain. The main stumbling block is the so called Courant limit[1] which requires unrealistically small time steps for progressing in time.

In this work package, the transient regime is addressed by implicit methods. This means that a time step is integrated using both the end-point as well as the begin point of the time interval. Our method is inspired by the transient simulation technique which is used in Technology Computer Aided Design (TCAD). In particular, there a backward finite difference is combined with the trapezoidal rule, leading to a rather enhanced time-step size.

The following topics will be discussed

- The electrical scalar potential V and the magnetic vector potential $\mathbf{A}$. The computation of $\mathbf{A}$ is complicated by the singular character of the equation for $\mathbf{A}$, leading to the requirement of a gauge condition.
- The discretization scheme demands that variables are placed on grid entities. Here, we present the method that the following grid entities contain fundamental variables: nodes contain the scalar potential V, and the semiconductor variables p, n or ϕ_p, ϕ_n. The links contain the fundamental variable $A = \mathbf{A} \cdot \mathbf{n}$, that means A is the projection of the vector potential along the link direction $\mathbf{n}$.
- The ports of the simulation structure, are excited by circuits. Therefore, the set of all equations for the field system is extended with a set of equations that control the port conditions or boundary conditions.
- The material interface conditions must be analysed in the time domain.

The following risks were identified:

- Can we stay consistent with causality requirements?
- Is the final system of linear equations solvable by iterative methods ?

A first technical approach consists of the following scheme. Using the MAGWEL solver, the matrices for the the system-state equations are exported. This system is extended with the circuit equations and the combined system is solved. Of particular interest is the feed-back loop. We consider first field systems that are linear in the time-differential operator. That means that a single system dump suffices for addressing the combined field-circuit problem. After having this problem settled, the more generic approach will be addressed where variables depend in a non-linear way on the state variables. These cases occur when semi-conductors are present.

[1] condition for convergence while solving certain PDEs numerically, arises when using explicit time-stepping methods.

2 Goals

The goal of WP3 is to give accurate simulation support to the model developers in WP1 and WP2 concerning device behavior in the transient regime. Whereas the frequency regime has already been developed in a rather advanced stage in earlier projects, the transient regime so far was not developed. The need for simulations in the transient regime comes from the desire to handle large-signal response. The following topics consists of a break down of sub tasks that will be addressed.

2.1 Implementation of adaptive time stepping methods

With Finite Difference Time Domain (FDTD) methods one is forced to fix a time step. However, here we can use variable time steps. Combinations of Runga-Kutta, trapazoidal rules backward-finite difference will be explored as well as predictor-corrector pairs (Bulirsch-Stoer).

2.2 The electromagnetic (EM) drift-diffusion (DD) solver in the time domain.

The MAGWEL software is build as a reusable, strongly object-oriented C++-code. The front-end needs only minor modification to set up the time domain control. The meshing algorithms can be fully reused. With these advantages in mind, it make sense to exploit these advantages. In particular, we can not only reuse the front-end but also the equation assembling can be done by reusing the algorithms for constructing the various terms. The next lines given an illustration how the MAGWEL code is internally organized to assemble an equation as a loop over mesh cells and for each cell, a term must be composed:

```
for(Mesh::Const_VolumeIterator cube = m_mesh->beginVolume();
cube != m_mesh->endVolume(); cube++)
{
        // find the cube material
        Material *cubematerial = cube->getData()->getMaterial();
        SEMIVOLUME  = cubematerial->isSemiconductor();
        METALVOLUME = cubematerial->isConductor();
        INSULVOLUME = cubematerial->isInsulator();

        // START OF THE MATRIX ASSEMBLING
        // Loop over all the nodes in the cube
        for(Volume::Const_NodeIterator node = cube->beginNode();
        node != cube->endNode(); node++)
        {
                // get info from the node
                nodeNumber = node->getNumber();
                // get the relevant data of the node
                nodeData = node->getData();

                bool METAL_SEMI = nodeData->isMetalSemiOrTriple();
                bool METAL_INSUL = nodeData->isMetalInsulOrTriple();

                // SEMICONDUCTOR VOLUME
```

```
                if (SEMIVOLUME)
                {
                     if (METAL_SEMI)
                        // CURRENT CONSERVATION
                        fillSemiCurrentContinuity(cube, node, row);
                     else
                       // POISSON EQUATION
                       fillSemiPoisson(cube, node,row);
                } // end if SEMIVOLUME

                // METAL VOLUME
                if (METALVOLUME)
                {
                      fillMetalCurrentContinuity(cube, node, row);
                } // end if METAL VOLUME

                // INSULATOR VOLUME
                if (INSULVOLUME)
                {
                        fillInsulPoisson(cube, node,row);
                } // end if INSULVOLUME

        } // end of node looping
} // end of cube looping
```

The piece of code illustrates the reuse of the architecture. New equations can be assembled fast by referring to the mesh and data structure, that is already present in STL (standard-template library) descriptions using containers and iterators.

3 WP3 Program

In this section we present the approach that is followed in this work package. In particular, the underlying equations that need to be considered are presented here as well as the strategy to solve these equations.

3.1 Circuit equations

The Modified Nodal Analysis (MNA) equations of an electrical circuit containing resistors, capacitors, inductors and independent voltage and current sources, which are not described by Maxwell's equations, have the form

$$A_C \frac{\mathrm{d}}{\mathrm{d}t} q_C(A_C^\mathsf{T} e, t) + A_R g_R(A_R^\mathsf{T} e, t) + A_L j_L + A_V j_V + A_I i_s(t) = 0, \tag{1a}$$

$$\frac{\mathrm{d}}{\mathrm{d}t} \phi(j_L, t) - A_L^\mathsf{T} e = 0, \tag{1b}$$

$$A_V^\mathsf{T} e - v_s(t) = 0, \tag{1c}$$

where A_C, A_R, A_L, A_V and A_I are the element related reduced incidence matrices. They describe the branch-node relationships for capacitors, resistors, inductors, voltage sources and current sources respectively. The independent variable $t \in [t_a,\, t_b]$ represents the time.

The unknowns are the node potentials, excepting the mass node $e(t) : \mathbb{R} \to \mathbb{R}^{n_N - 1}$ and the currents through inductors and voltage sources $j_L(t) : \mathbb{R} \to \mathbb{R}^{n_L}$ and $j_V(t) : \mathbb{R} \to \mathbb{R}^{n_V}$ respectively, where $n_N - 1$ represents the number of nodes (excepting the mass node) in the directed graph associated to the circuit, n_L is the number of capacitive branches in this graph and n_V, the number of branches that correspond to voltage sources.

Equations (1a) are the Kirchoff's current law equations for the circuit and Equations (1b)-(1c) describe its inductors and voltage sources. In particular, Equations (1c) are the Kirchoff's voltage law equations for the voltage sources in the circuit.

An initial value $(t_a, e_a, j_{La}, j_{Va})$ for (1) is called *consistent* if there is a solution of (1) that fulfills $e(t_a) = e_a,\ j_L(t_a) = j_{La},\ j_V(t_a) = j_{Va}$.

In order to bridge the communication between the world of circuit simulation, we explain the terminology that is used in both environments. The voltage, e, are known in the field solver as V provided that they are located at metal or insulator field nodes. If the the latter nodes are attached to semiconductor nodes, i.e. the node is intrinsic semi conductor or on a semiconductor/insulator interface, it is identified with the Fermi potential. For nodes that are located at the semiconductor/metal interface, the voltage e is identified with the voltage $V|_{metal}$. Note that the potential makes a discrete jump when moving from the metal into the semiconductor.

3.1.1 Example of MNA of a simple circuit

In this paragraph we will illustrate the model analysis with a simple example. The purpose of this paragraph is to show the MNA 'in action'. In Fig. 2, we show the variables of a simple RC network. The example is borrowed from "wikipedia".

The circuit has two nodes which are marked as red spots. Each nodes introduces a nodal voltage e_i into the nodal analysis. There a three currents in the circuit. Each branch generates

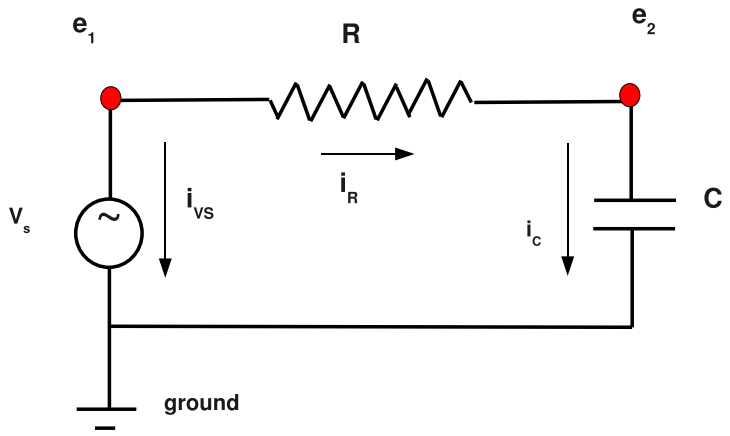

Figure 1: Elementary circuit for illustrating MNA.

its own current. The currents are i_{VS}, i_R, i_C. At the nodes we apply the Kirchhoff current laws (KCL):

- At node #1: $i_{VS} + i_R = 0$
- At node #2: $-i_R + i_C = 0$

Besides the KCL we have to set up the branch-constituent equations (BCE). There are three branches, leading to

- At branch for i_{VS}: $V_S = e_1$
- At branch for i_R: $V_R = e_1 - e_2$
- At branch for i_C: $V_C = e_2$

Next we will need the voltage-current characteristics of the elements:

- For the resistor: $V_R = R\, i_R$
- For the capacitance: $i_C = C\frac{\mathrm{d}V_C}{\mathrm{d}t}$

The modified nodal analysis collects all equations for $\{i_i, e_i\}$. Here we have 5 unknowns. The full problem can be casted into the following form. Let $\mathbf{x}(t)$ be the collection of unknowns. Then the system is fully described by the following differential-algebraic equation :

$$\mathbf{A} * \frac{\mathrm{d}}{\mathrm{d}t}\mathbf{x}(t) + \mathbf{B} * \mathbf{x}(t) + \mathbf{f} = 0 \tag{2}$$

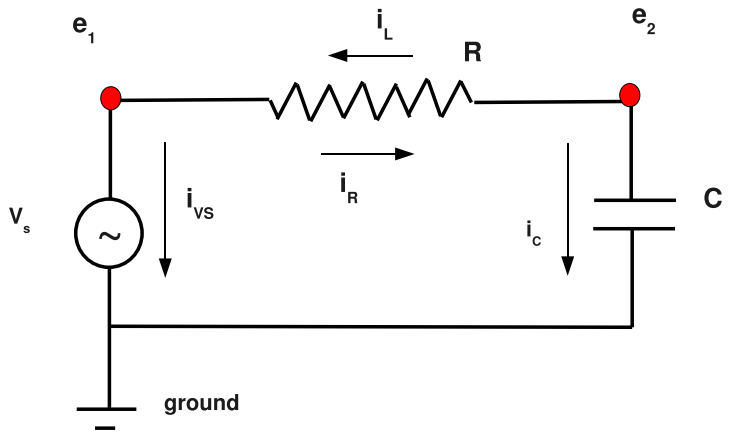

Figure 2: Elementary circuit for illustrating MNA with nodal-perspective currents.

The entries in equation (2) are :

$$\mathbf{x}(t) = \begin{bmatrix} i_{VS} \\ i_R \\ i_C \\ e_1 \\ e_2 \end{bmatrix} \quad \mathbf{f} = \begin{bmatrix} 0 \\ 0 \\ 0 \\ 0 \\ -V_S \end{bmatrix} \quad \mathbf{A} = \begin{bmatrix} 0 & 0 & 0 & 0 & 0 \\ 0 & 0 & 0 & C & 0 \\ 0 & 0 & 0 & 0 & 0 \\ 0 & 0 & 0 & 0 & 0 \\ 0 & 0 & 0 & 0 & 0 \end{bmatrix} \quad \mathbf{B} = \begin{bmatrix} 0 & -R & 0 & 1 & -1 \\ 0 & 0 & -1 & 0 & 0 \\ 1 & -1 & 0 & 0 & 0 \\ 0 & -1 & 1 & 0 & 0 \\ 0 & 0 & 0 & 1 & 0 \end{bmatrix} \tag{3}$$

We can easily eliminate the variables i_R and i_C leading to a system for 3 unknowns. On the contrary, we want to modify the problem formulation and *extend* the number of unknowns. For that purpose, we review Fig. 2. The current through the resistor will be described once from the left-node perspective and once from the right-node perspective. The equation $i_R R + e_1 - e_2 = 0$, is complementary to the equation $i_L R + e_2 - e_1 = 0$. Of course, all that is added is a new trivial variable $i_L = -i_R$. However, although this knowledge is known for this simple example, before doing any computation, we can anticipate circumstances where such knowledge can only be obtained after an elaborate computation. For example, $i_L = i_R$ may be the result of a complicated resistive network representing R. The extension shows that part of the MNA can be an impedance matrix at some location in the net list.

$$\begin{bmatrix} i_R \\ i_L \end{bmatrix} = \begin{bmatrix} 1 & -1 \\ -1 & 1 \end{bmatrix} * \begin{bmatrix} e_1 \\ e_2 \end{bmatrix} = \mathbf{Y} * \begin{bmatrix} e_1 \\ e_2 \end{bmatrix} \tag{4}$$

and $\mathbf{Y}$ is the admittance matrix.

Thus from this elementary example we can already extract quite some insight how to couple circuit simulators and field solvers. For each contact pad of the field solver we assign a voltage and current variable. All these voltage and current variables will be loaded into the state vector of the modified-nodal analysis. Suppose that there are n contact pads. (They may be organised

in $n/2$ ports.) Then there are $2n$ variables entering the MNA. We should not a priori demand that the total current is zero. This is obtained as a consequence of solution from the field solver.

3.2 EM-DD equations

Note: In this section, we will present our equations as $lhs = rhs$, for didactic reason. In a later stage we will collect our results as $lhs = 0$, for computational reasons.

3.2.1 Use of potentials

Our starting point will be the equations of Maxwell:

$$\text{Gauss' law:} \quad \nabla \cdot \mathbf{D} = \rho \tag{5}$$

$$\text{Absence of magnetic monopoles:} \quad \nabla \cdot \mathbf{B} = 0 \tag{6}$$

$$\text{Maxwell-Faraday:} \quad \nabla \times \mathbf{E} = -\frac{\partial \mathbf{B}}{\partial t} \tag{7}$$

$$\text{Maxwell-Ampère:} \quad \nabla \times \mathbf{H} = \mathbf{J} + \frac{\partial \mathbf{D}}{\partial t} \tag{8}$$

where $\mathbf{D}$, $\mathbf{E}$, $\mathbf{B}$, $\mathbf{H}$, $\mathbf{J}$ en ρ are the electric induction, the electric field, magnetic induction and magnetic field, current density and charge density.

The following constitutive laws are used:

$$\mathbf{B} = \mu \mathbf{H}, \qquad \mathbf{D} = \varepsilon \mathbf{E} \tag{9}$$

The charge density ρ and current density $\mathbf{J} = 0$ in insulating materials and charge density ρ consists of a fixed background charge. In conductive domains we rely on the current continuity:

$$\nabla \cdot \mathbf{J} + \frac{\partial \rho}{\partial t} = 0 \tag{10}$$

If these conductive domains are metallic, then we apply Ohm's law for the connection between electric field intensity and current density. It should be noted that this is not the most general expression and for Hall devices a magnetic field dependence must also be included. However, here we limit ourselves to situations where the magnetic fields are sufficiently weak in order to ignore Hall currents:

$$\mathbf{J} = \sigma \mathbf{E} \tag{11}$$

It should also be noted that the charge density and current densities are determined by the physical character of the materials under study. For example leakage currents can flow in insulating layers and the current-field relation is highly non-linear since tunneling mechanisms play an important role. Semiconductors also have more general current-field relations as given above and these will be discussed later.

We introduce the scalar potential V en the magnetic vector potential $\mathbf{A}$ that satisfy

$$\mathbf{B} = \nabla \times \mathbf{A} \tag{12}$$

$$\mathbf{E} = -\nabla V - \frac{\partial \mathbf{A}}{\partial t} \tag{13}$$

then the Maxwell equation become in these variables;

- *for insulators:*

$$-\nabla \cdot \left[\varepsilon \left(\nabla V + \frac{\partial \mathbf{A}}{\partial t}\right)\right] = 0 \quad (14)$$

$$\nabla \times \frac{1}{\mu}\left(\nabla \times \mathbf{A}\right) = -\varepsilon \frac{\partial}{\partial t}\left(\nabla V + \frac{\partial \mathbf{A}}{\partial t}\right) \quad (15)$$

- *for conductors:*

$$-\nabla \cdot \sigma \left(\nabla V + \frac{\partial \mathbf{A}}{\partial t}\right) = \frac{\partial}{\partial t}\left(\nabla \cdot \varepsilon \left(\nabla V + \frac{\partial \mathbf{A}}{\partial t}\right)\right) \quad (16)$$

$$\nabla \times \frac{1}{\mu}\left(\nabla \times \mathbf{A}\right) = -\sigma \left(\nabla V + \frac{\partial \mathbf{A}}{\partial t}\right) - \varepsilon \frac{\partial}{\partial t}\left(\nabla V + \frac{\partial \mathbf{A}}{\partial t}\right) \quad (17)$$

For the description in the Fourier domain we replace each differentiation w.r.t. time by a factor $j\omega$, with j the imaginary unit and $\omega = 2\pi f$ the angular velocity and f is the operational frequency.

These differential equations are with the MAGWEL software discretized in 3D-space using the finite-volume method (FVM) and finite-surface method (FSM). Whereas the FVM is based on averaging variables over cells to obtain discrete variables the FSM averages method obtains discrete variables by averaging over surfaces. These averaging procedures apply Gauss' law (FVM) and Stokes' law (FSM). The success of the method is based on respecting the geometrical origin of the various variables that are encountered in the mathematical set up.

For the description in the time domain we can reuse the spatial discretization methods. However, we will end up with a second-order differentiation in time. Part of the research in this WP will be to give a procedure for a correct treatment of these terms. Physically, the second order time-derivative terms illustrate the wave delay that is found in the Maxwell equations. A popular argument for handling these terms is based on considering the scales of application. In particular, if we are operating in the below 100 GHz range, the wave length is 3 mm=3000 microns. Assuming that typical lengths inside the chip is below this figure, it is argued that these 2nd order time derivatives could be ignored. Thus a 'crude' method just ignores the second order time differential on $\mathbf{A}$. As a consequence we arrive at some form of a quasi-static approximation and one is not accounting for the delay induced by wave propagation. Another way of looking at this approximation is to assume that speed of light is infinity. In the PEEC method this approximation is exploited *PEEC* (Partial Element Equivalent Circuit Method).

Dropping terms out of equations should be done with care. Although a term may seem irrelevant on an instantaneous view, it must be considered also from the view how it participates in keeping the global behavior physically correct. For instance, spontaneous creation of charge is prohibited and dropping one term might induce the need to drop corresponding terms for physical consistency. In order to explore these pitfalls, we propose another representation.

The second approach introduces a new variable the *pseudo-canonical momentum* $\Pi = \partial \mathbf{A}/\partial t$. We may rewrite the system of equations as (e.g. for a conductor):

$$-\nabla \cdot \sigma \left(\nabla V + \mathbf{\Pi}\right) = \nabla \cdot \varepsilon \left(\nabla \frac{\partial V}{\partial t} + \frac{\partial \mathbf{\Pi}}{\partial t}\right) \quad (18)$$

$$\nabla \times \left(\frac{1}{\mu}\nabla \times \mathbf{A}\right) = -\sigma \left(\nabla V + \frac{\partial \mathbf{A}}{\partial t}\right) - \varepsilon \left(\nabla \frac{\partial V}{\partial t} + \frac{\partial \mathbf{\Pi}}{\partial t}\right) \quad (19)$$

$$\mathbf{\Pi} = \frac{\partial \mathbf{A}}{\partial t} \quad (20)$$

We refer to the variable $\mathbf{\Pi}$ as a *pseudo*-canonical momentum, because when deriving the field equations from an Lagrange action, the electric field $-\mathbf{E}$ is found as the canonical conjugate to $\mathbf{A}$. The difference between the pseudo-canonical momentum and the canonical momentum is

$$\mathbf{\Pi} = -\mathbf{E} - \nabla V \tag{21}$$

3.2.2 Gauge conditions

The Equations (155-17) do not uniquely determine $\mathbf{A}$ and V. A solution can be $\mathbf{A}$, V can be adapted with a arbitrary scalar field χ

$$\begin{aligned} \mathbf{A}^{'} &= \mathbf{A} + \nabla\chi \\ V^{'} &= V - \frac{\partial\chi}{\partial t} \end{aligned}$$

which results into an equally valid solution of (155-17). After discretization the coefficient-matrix is singular. Additional equations must be added to elevate this singularity. These extra equations are the gauge conditions.

For the Coulomb gauge the following constraint is applied:

$$\nabla \cdot \mathbf{A} = \mathbf{0} \tag{22}$$

The Lorentz gauge is inspired by dealing with the term $\epsilon\nabla\left(\frac{\partial V}{\partial t}\right)$ in the Ampere-Maxwell equation:

$$\frac{1}{\mu}\,\nabla\left(\nabla \cdot \mathbf{A}\right) + \epsilon\nabla\left(\frac{\partial V}{\partial t}\right) = 0 \tag{23}$$

Usually we encounter the Lorenz gauge condition as

$$\nabla \cdot \mathbf{A} + \mu\epsilon\frac{\partial V}{\partial t} = 0 \tag{24}$$

However, we prefer to keep it in the form (23) because we need it in this way and moreover the form (24) is only equivalent to (23) for μ and ϵ constant. The pre-factor $1/\mu$ is a choice which is convenient in our field of application (EDA). We are dealing mostly with materials that are not ferromagnetic. Then $\mu_r = 1$, which allows an efficient evaluation of the Maxwell-Ampere equation.

Above argument is somewhat 'naive'. Actually, we do skip two terms in the Ampere-Maxwell equation by first adding and subtracting $1/\mu\nabla\left(\nabla \cdot \mathbf{A}\right)$ and use one to regularize the double curl operator.

For later use, we write the Lorentz gauge condition as

$$\epsilon\nabla\left(\frac{\partial V}{\partial t}\right) = -\,\frac{1}{\mu}\,\nabla\left(\nabla \cdot \mathbf{A}\right) \tag{25}$$

The Maxwell-Ampere equation can be written as

$$\epsilon\frac{\partial \mathbf{\Pi}}{\partial t} = -\nabla \times \left(\frac{1}{\mu}\nabla \times \mathbf{A}\right) + \frac{1}{\mu}\nabla\left(\nabla \cdot \mathbf{A}\right) - \sigma\nabla V - \sigma\mathbf{\Pi} \tag{26}$$

Furthermore, remember that

$$\frac{\partial \mathbf{A}}{\partial t} = \mathbf{\Pi} \tag{27}$$

then we arrive at the following condensed notation for the transient description

$$\varepsilon \frac{\partial}{\partial t} \begin{bmatrix} V \\ \mathbf{A} \\ \mathbf{\Pi} \end{bmatrix} = \mathcal{K} * \begin{bmatrix} V \\ \mathbf{A} \\ \mathbf{\Pi} \end{bmatrix} + \mathcal{B} * \begin{bmatrix} V_{dbc} \\ \mathbf{A}_{dbc} \\ \mathbf{\Pi}_{dbc} \end{bmatrix} \tag{28}$$

where $\mathcal{K}$ is a 3x3 matrix that can be generated in the MAGWEL solver, and $\mathcal{B}$ is an operator acting on the boundary-condition prescribed values. The $V_{dbc}, \mathbf{A}_{dbc}$ and $\mathbf{\Pi}_{dbc}$ are given values Dirichlet boundaries. In Section 4, examples are given.

The $\mathcal{K}$ matrix represents the following operators:

$$\mathcal{K} = \begin{bmatrix} 0 & -\frac{1}{\mu}\nabla\cdot & 0 \\ 0 & 0 & \epsilon \\ -\sigma\nabla & -\nabla\times\,[\frac{1}{\mu}\nabla\times\ \ ] + \frac{1}{\mu}\nabla\,[\nabla\cdot\ \ ] & -\sigma \end{bmatrix} \tag{29}$$

It should be noted that a formal solution exists that can be found by the method of 'variations of constants'. The solution is

$$\begin{bmatrix} V \\ \mathbf{A} \\ \mathbf{\Pi} \end{bmatrix} = \int_0^t \mathrm{d}t' \mathrm{e}^{\frac{\mathcal{K}}{\varepsilon}(t-t')} \ * \ \frac{\mathcal{B}}{\varepsilon} * \begin{bmatrix} V_{dbc}(t') \\ \mathbf{A}_{dbc}(t') \\ \mathbf{\Pi}_{dbc}(t') \end{bmatrix} + \begin{bmatrix} V_0 \\ \mathbf{A}_0 \\ \mathbf{\Pi}_0 \end{bmatrix} \tag{30}$$

where the last represents the field configuration at $t = 0$. An interesting case corresponds to switch-on response. In that case the initial solution is zero and the boundary terms are :

$$\begin{bmatrix} V_{dbc}(t) \\ \mathbf{A}_{dbc}(t) \\ \mathbf{\Pi}_{dbc}(t) \end{bmatrix} = \begin{bmatrix} V_{dbc} \\ \mathbf{A}_{dbc} \\ \mathbf{\Pi}_{dbc} \end{bmatrix} \Theta(t) \tag{31}$$

and $\Theta(t)$ is the step function. Then the solution is :

$$\begin{bmatrix} V \\ \mathbf{A} \\ \mathbf{\Pi} \end{bmatrix} (t) = \mathcal{K}^{-1} * \left(1 - \mathrm{e}^{\frac{\mathcal{K}}{\epsilon}t}\right) * \mathcal{B} * \begin{bmatrix} V_{dbc} \\ \mathbf{A}_{dbc} \\ \mathbf{\Pi}_{dbc} \end{bmatrix} \tag{32}$$

Note that in the evolution of the system, the gauge condition is needed to describe the time dependence of V. Quite remarkably, the Gauss' equation is not used for that purpose. Gauss' law can be written as

$$\mathcal{G} * \begin{bmatrix} V \\ \mathbf{A} \\ \mathbf{\Pi} \end{bmatrix} = \mathcal{Q} \tag{33}$$

The $\mathcal{G}$ matrix is represented by the 1×3 operator :

$$\mathcal{G} = \ \left[\ \nabla[-\epsilon[\nabla\ ]]\ ,\quad 0\ ,\quad -\nabla[\epsilon\ \ ]\ \right] \tag{34}$$

In more familiar language:

$$\nabla \cdot [\epsilon\,(-\nabla V - \mathbf{\Pi})] = \rho \tag{35}$$

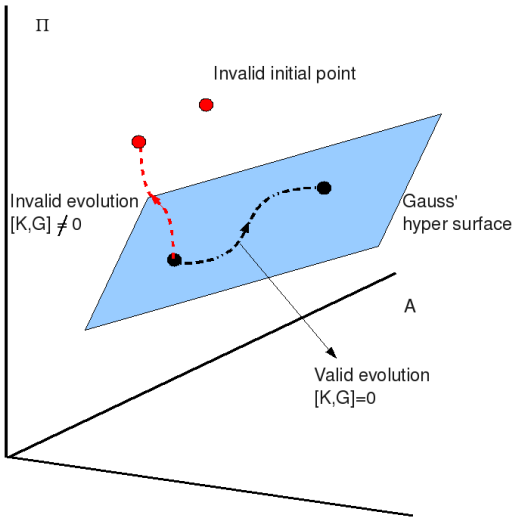

Figure 3: Illustration of the use of Gauss' law.

Gauss' law is a constraint between 'canonical' coordinates and momenta. Every update from one time instant to the next must be compliant with this constraint. In order to have a correct physical evolution it is needed that the Gauss' law is also obtained after a forward sweep in time. We suspect that this is guaranteed if the operators $\mathcal{K}$ and $\mathcal{G}$ commute. Thus a discrete implementation requires that

$$[\mathcal{K}, \mathcal{G}] = 0 \tag{36}$$

The discretization procedure generates explicit expression for the matrices $\mathcal{K}$ and $\mathcal{G}$ and therefore their commutation can be checked.

It is important to realize that a *transient* simulator solves the temporal evolution in terms of:

- The *gauge condition* for computing the changes in time of V
- The *definition* of the pseudo-canonical momentum $\mathbf{\Pi}$ for computing the changes in time of $\mathbf{A}$
- The *Maxwell-Ampere equation* for computing the changes in time of $\mathbf{\Pi}$.
- Gauss law does *not* play a role for determining the time-evolution, but informs us that we can not start from an arbitrary $(V, \mathbf{A}, \mathbf{\Pi})$ - configuration, but one that satisfies Gauss' law.

The last item is illustrated in Fig. 3. In the $(V, \mathbf{A}, \mathbf{\Pi})$ - configuration space there is a hyper surface compliant with Gauss' law. An initial point should be located at this hyper surface. Next the time-evolution operator $\mathcal{K}$ should guarantee that the flow remains on this hyper surface.

3.2.3 Semiconductor treatment

For the simulation of semiconductor regions we use the current-continuity equations

$$\nabla \cdot \mathbf{J}_{\mathrm{n}} - q\frac{\partial n}{\partial t} = U(n,p), \tag{37}$$

$$\nabla \cdot \mathbf{J}_{\mathrm{p}} + q\frac{\partial p}{\partial t} = -U(n,p). \tag{38}$$

Here, n and p are the electron and hole concentrations and $U(n,p)$ represent the generation/recombination mechanisms. The drift-diffusion model provides us with explicit relations between the electron and hole current densities and the electric field intensity as well as the carrier concentration

$$\mathbf{J}_{\mathrm{n}} = q\mu_{\mathrm{n}} n\mathbf{E} + qkT\mu_{\mathrm{n}}\nabla n, \tag{39}$$

$$\mathbf{J}_{\mathrm{p}} = q\mu_{\mathrm{p}} p\mathbf{E} - qkT\mu_{\mathrm{p}}\nabla p. \tag{40}$$

The charge density ρ is

$$\rho = q(p - n + N_{\mathrm{D}} - N_{\mathrm{A}}) \tag{41}$$

The carrier concentrations are modeled using the Boltzmann distribution, i.e. the amount of carriers with a given amount of energy is proportional to the exponential of the $-E/kT$. Introducing the Fermi potentials ϕ_n and ϕ_p the following relation holds:

$$n = n_i\, \mathrm{e}^{\frac{q}{kT}(V-\phi_n)}, \qquad p = n_i\, \mathrm{e}^{\frac{q}{kT}(\phi_p - V)},$$

and n_i is the intrinsic carrier concentration.

We can add the following set of equations for the description of semiconductors (153-17)

$$-\nabla\cdot\varepsilon\left(\nabla V + \frac{\partial \mathbf{A}}{\partial t}\right) = qn_i\, \mathrm{e}^{\frac{q}{kT}(\phi_p - V)} - qn_i\, \mathrm{e}^{\frac{q}{kT}(V-\phi_n)} + N_{\mathrm{D}} - N_{\mathrm{A}} \tag{42}$$

$$\begin{aligned}\nabla \times \frac{1}{\mu}(\nabla \times \mathbf{A}) = {} & q\mu_p n_i\, \mathrm{e}^{\frac{q}{kT}(\phi_p - V)}\left(\nabla V + \frac{\partial \mathbf{A}}{\partial t}\right) - qkT\mu_p \nabla n_i e^{\frac{q}{kT}(\phi_p - V)} \\ & + q\mu_n n_i\, \mathrm{e}^{\frac{q}{kT}(V-\phi_n)}\left(\nabla V + \frac{\partial \mathbf{A}}{\partial t}\right) + qkT\mu_n \nabla n_i e^{\frac{q}{kT}(V-\phi_n)} \\ & - \varepsilon\frac{\partial}{\partial t}\left(\nabla V + \frac{\partial \mathbf{A}}{\partial t}\right)\end{aligned} \tag{43}$$

$$\begin{aligned}\nabla\cdot\left(q\mu_p\, n_i \mathrm{e}^{\frac{q}{kT}(\phi_p - V)}\left(\nabla V + \frac{\partial \mathbf{A}}{\partial t}\right) - qkT\mu_p \nabla e^{\frac{q}{kT}(\phi_p - V)}\right) = {} & -U(n,p) \\ & - qn_i\frac{\partial}{\partial t}\left(\mathrm{e}^{\frac{q}{kT}(\phi_p - V)}\right)\end{aligned} \tag{44}$$

$$\begin{aligned}\nabla\cdot\left(q\mu_n\, n_i \mathrm{e}^{\frac{q}{kT}(V-\phi_n)}\left(\nabla V + \frac{\partial \mathbf{A}}{\partial t}\right) + qkT\mu_n \nabla e^{\frac{q}{kT}(V-\phi_n)}\right) = {} & U(n,p) \\ & + qn_i\frac{\partial}{\partial t}\left(e^{\frac{q}{kT}(V-\phi_n)}\right)\end{aligned} \tag{45}$$

We have presented here all expressions explicitly in terms of the potentials in order to illustrate the non-linear character of the equation system.

The set of unknowns $(V, \mathbf{A}, \mathbf{\Pi})$ needs to be extended with the Fermi levels ϕ_p and ϕ_n or alternatively with p and n. In this case we can add the following set of equations for the description of semiconductors (153-17)

$$
\begin{aligned}
-\nabla \cdot \varepsilon \left(\nabla V + \frac{\partial \mathbf{A}}{\partial t} \right) &= q(p-n) + N_{\mathrm{D}} - N_{\mathrm{A}} && (46)\\
\nabla \times \frac{1}{\mu} (\nabla \times \mathbf{A}) &= \underbrace{-q\mu_p p \left(\nabla V + \frac{\partial \mathbf{A}}{\partial t} \right) - qkT\mu_p \nabla p}_{:=\mathbf{J}_p} && (47)\\
& \underbrace{-q\mu_n n \left(\nabla V + \frac{\partial \mathbf{A}}{\partial t} \right) + qkT\mu_n \nabla n}_{:=\mathbf{J}_n} && (48)\\
& -\varepsilon \frac{\partial}{\partial t} \left(\nabla V + \frac{\partial \mathbf{A}}{\partial t} \right) && (49)\\
\nabla \cdot \left(q\mu_p p \left(\nabla V + \frac{\partial \mathbf{A}}{\partial t} \right) - qkT\mu_p \nabla p \right) &= -U(n,p) - q\frac{\partial p}{\partial t} && (50)\\
\nabla \cdot \left(q\mu_n n \left(\nabla V + \frac{\partial \mathbf{A}}{\partial t} \right) + qkT\mu_n \nabla n \right) &= U(n,p) + q\frac{\partial n}{\partial t} && (51)
\end{aligned}
$$

In the frequency domain we have linearized the equation at some operation point

$$X_{op} = (\mathbf{E}_0, p_0, n_0) \tag{52}$$

$$
\begin{aligned}
\mathbf{J}_{\mathrm{n}} &= q\mu_{\mathrm{n}} n_0 \mathbf{E} + q\mu_{\mathrm{n}} n \mathbf{E}_0 + qkT\mu_{\mathrm{n}} \nabla n && (53)\\
\mathbf{J}_{\mathrm{p}} &= q\mu_{\mathrm{p}} p_0 \mathbf{E} + q\mu_{\mathrm{p}} p \mathbf{E}_0 - qkT\mu_{\mathrm{p}} \nabla p, && (54)
\end{aligned}
$$

where the operation point is determined by a solution of the static bias conditions $(\mathbf{E}_0, p_0, n_0)$. In the time domain, we are interested in a direct integration in time to explore the solution. Linearization methods will have only restricted value.

4 Implementation of numerical methods for solving the equations

4.1 Introduction

The discretization procedure will be separated into two parts. First we will described the handling of the fields on the discrete spatial grid. After the spatial discretization, we have transform our problem definition from having a finite set of fields $\psi_n(\mathbf{x}, t)$ to a lattice of variables $\psi_{n,k}(t)$, where n is an index to the field under consideration e.g. $V, \mathbf{A}, \phi_p, \phi_n$ and k labels a grid object, i.e. a node or a link. So far each variable is still a continuous function of time. In the second part, we will discuss how the transient problem will be numerically addressed.

4.2 Spatial discretization

In order to solve the continuous partial differential equations a transition must be made to a discretization grid. How this is done in general is well-known in the literature. Here, we will emphasize the main ingredients as well as the subtle details that come with our specific set of equations under consideration.

A convenient mental picture is to address the discretization in three steps: First we replace the continuous 'universe' by a lattice of discrete points. Next we replace the continuous differential operators by local coupling between neighboring lattice points, and thirdly, we cut out of the 'entire universe' a finite portion and give conditions (usually idealized ones) how the rest of universe interferes with the portion under consideration. We refer to this finite portion as the simulation domain, Ω which has an enclosing surface $\partial\Omega$. In a nutshell this is what discretization is about. Already right at the start we encounter a subtle detail. Cutting out a piece out of large geometrical entity and remembering that our starting equations have a local character, it would mean that the impact of the external domain would take place only via the surface of the simulation domain. In other words boundary conditions are expected on the surface $\partial\Omega$. Although this makes sense from a mathematical perspective, it has been shown beneficial to allow for 'internal' boundary conditions also. Since the external part is not part of our computation problem ("by definition") all the lattice variables are corresponding to this part have no representation in the computer memory. There presence is absorbed in a series of restrictions for the lattice variables of the internal, i.e. those variables that have a chunk of memory allocated. Within this view, one may consider boundary conditions as a set of limitations to construct a solvable problem only the word 'boundary' should not be taken too literally.

4.2.1 Discretization of Gauss' law

As an illustration of the discretization method, we will here discretize Gauss' law [2]. The starting equation is

$$-\nabla\left[\epsilon\left(\nabla V + \frac{\partial \mathbf{A}}{\partial t}\right)\right] - \rho = 0 \tag{55}$$

On a discretization grid we consider the Voronoi cells around each node, say i, of the grid and

[2] It should be emphasized that the purpose of this section is to show typical discretization steps. Remember that the role of Gauss' law is to provide constraints on the initial values and that the time evolution should be compliant with it.

take take the volume integral of equation (55). Applying Gauss' law we find that

$$\int_{\partial(\Delta v)} \mathbf{dS} \cdot (-\epsilon) \left(\nabla V + \frac{\partial \mathbf{A}}{\partial t} \right) - Q(\Delta v) = 0 \tag{56}$$

Using the geometrical information of the Voronoi cells this amounts to adding all contribution from each link that ends or begins in node i

$$\sum_j \epsilon \left[\frac{S_{ij}}{h_{ij}} (V_i - V_j) - \sigma_{ij} \frac{\mathrm{d}A_{ij}}{\mathrm{d}t} S_{ij} \right] - Q_i = 0. \tag{57}$$

In this expression, the sum j is over all neighboring nodes. S_{ij} is the perpendicular area for the link connecting node i and node j. The variable h_{ij} is the length of the link ij. Furthermore, A_{ij} is the projection of the vector potential on link (ij) and is also a degree of freedom. The variable $\sigma_{ij} = \pm 1$. It represents the relative orientation of the vector potential with respect to the grid orientation.

4.2.2 Boundary conditions for Gauss' discretized law

We are now in the position to consider the boundary conditions for above set of equations. Let $\mathcal{N}_\infty$ be the collection of all lattice nodes and links for the 'universe', let $\mathcal{N}_{sim}$ be the collection of all lattice nodes and link that participate in the simulation problem. How can we get rid off $\mathcal{N}_\infty - \mathcal{N}_{sim}$? A simple idea is that there are parts of the surface of the simulation domain where the interaction is not present. This means that the perpendicular displacement at $\partial\Omega$ is zero, i.e $\mathbf{D}.\mathbf{n} = 0$. As a consequence, we can assemble (57) just as if the the rest of the universe does not exists. The assembling is illustrated in the introduction. This approach is known as putting Neumann boundary conditions.

Another elimination procedure is to assume that the impact of the rest of the universe is screened off by prescribed values at (other) segments of $\partial\Omega$. Voltage sources are a physical realization. These are the Dirichlet's boundary conditions.

We can now consider equation (57) in more detail. Actually as it stands it reads as follows:

$$\sum_j \epsilon \left[\frac{S_{ij}}{h_{ij}} (V_i - V_j) - \sigma_{ij} \frac{\mathrm{d}A_{ij}}{\mathrm{d}t} S_{ij} \right] - Q_i = 0 \qquad\qquad i \subset \mathcal{N}_\infty \tag{58}$$

This is now further specified as follows: The set $\mathcal{N}_{sim}$ consists of two groups. The first set contains the true degrees of freedom. We refer to this set as $\mathcal{N}_{sim}^{dof}$. The second set contains the Dirichlet boundary condition set, denoted as $\mathcal{N}_{sim}^{dbc}$. Let us also introduce a notational convenience: time derivatives will be denoted with a dot.

$$\sum_j \epsilon \left[\frac{S_{ij}}{h_{ij}} (V_i - V_j) - \sigma_{ij} \dot{A}_{ij} S_{ij} \right] - Q_i = 0 \qquad\qquad i \subset \mathcal{N}_{sim}^{dof} \tag{59}$$

Next we can consider the sum at the left-hand side. For each degree-of-freedom, we can separate the sum into two sets also. The first set contains the coupling to other degrees of freedom ('internal' nodes) and the second set contains the coupling to the Dirichlet boundary

nodes. Thus we obtain

$$\sum_{j\subset\mathcal{N}_{sim}^{dof}} \epsilon\left[\frac{S_{ij}}{h_{ij}}\left(V_i-V_j\right)-\sigma_{ij}\dot{A}_{ij}S_{ij}\right]+\sum_{j\subset\mathcal{N}_{sim}^{dbc}} \epsilon\left[\frac{S_{ij}}{h_{ij}}\left(V_i-V_j\right)-\sigma_{ij}\dot{A}_{ij}S_{ij}\right]-Q_i=0$$

$$i\subset\mathcal{N}_{sim}^{dof} \qquad (60)$$

Finally, the second sum can be split as shown below:

$$\sum_{j\subset\mathcal{N}_{sim}^{dof}} \epsilon\left[\frac{S_{ij}}{h_{ij}}\left(V_i-V_j\right)-\sigma_{ij}\dot{A}_{ij}S_{ij}\right]+V_i\sum_{j\subset\mathcal{N}_{sim}^{dbc}}\epsilon\frac{S_{ij}}{h_{ij}}$$

$$-\sum_{j\subset\mathcal{N}_{sim}^{dbc}}\sigma_{ij}\dot{A}_{ij}S_{ij}-Q_i \;=\; \sum_{j\subset\mathcal{N}_{sim}^{dbc}}\epsilon\frac{S_{ij}}{h_{ij}}V_j, \qquad i\subset\mathcal{N}_{sim}^{dof}$$

Recognizing all V_i as degrees of freedom and all V_j as prescribed values we see that the discretized system finally take the form:

$$\mathbf{A}*\mathbf{x}=\mathbf{b} \qquad (61)$$

Here, we assumed that ρ and therefore Q_i is independent of the voltages. For semiconductors being present this is not true, and we end up with a system that is non-linear in the voltages. Then Newton-Raphson schemes are needed to solve the full system.

We have not mentioned yet the detailed discretization for the projected vector potentials however, as for as the discussion for the Gauss' law is concerned, all A_{ij} are degrees of freedom. This is because the the links on $\partial\Omega$ have a simple Dirichlet-type boundary condition, $A_{ij}=0 \quad (ij)\subset\partial\Omega$. In fact, this matrix consists of two parts in this example. To be more precise, it takes the form[3]

$$\left(\mathbf{A}_0+\mathbf{A}_1\frac{\mathrm{d}}{\mathrm{d}t}\right)*\mathbf{x}=\mathbf{b} \qquad (62)$$

where $\mathbf{A}_1$ acts on the link degrees of freedom.

In a first phase of the project, we will make available the matrix $\mathbf{A}$ explicitly for linear problems. To be more precise; starting from the existing MAGWEL solver in the frequency domain, we can assemble the equations as is done for the harmonic analysis and extract explicitly the matrices $\mathbf{A}_0$ and $\mathbf{A}_1$. That means that no semiconductors are present in this phase. It also means that the matrices $\mathbf{A}$ can be used at all time steps (see next chapter).

The right-hand side will be made explicitly available as

$$\mathbf{b}=\mathbf{B}*\mathbf{u}, \qquad (63)$$

where $\mathbf{u}$ is a vector of size of the number of contacts to which voltages can be assigned and $\mathbf{B}$ is a matrix describing the right-hand side of (61). The number of rows is equal to the number of degrees of freedom. Furthermore, just as for $\mathbf{A}$, the matrix $\mathbf{B}$ can be extracted from MAGWEL's solver in for harmonic analysis.

The time derivative in (62) appears because we kept the variables in the basic representation. When transforming to the first-order formulation, the link variables $\dot{A}_{ij}$ will become equal to the canonical momenta assigned to the links, i.e.

$$\Pi_{ij}=\dot{A}_{ij} \qquad (64)$$

[3]Beware that this formulation is misleading! Writing down Gauss' law by making d/dt explicit, suggests that it represents a time evolution equation after all. However, it does not as is discussed below.

Thus Equation (62) can also be written as

$$\mathbf{A} * \mathbf{x} = \mathbf{b} \qquad \mathbf{x} = \begin{bmatrix} V_1 \\ \cdot \\ \cdot \\ V_i \\ \cdot \\ \cdot \\ \Pi_{12} \\ \cdot \\ \cdot \\ \Pi_{ij} \\ \cdot \\ \cdot \end{bmatrix} \tag{65}$$

This is in agreement with Equation (35) in which neither an explicit time differentiation is found. We will now proceed with the spatial discretization of the magnetic sector. For future considerations, we will introduce here a new notation. Instead of referring to a link variable A_{ij}, we will now work with a unique ID (identity) for each link which is an integer. A link degree-of-freedom will be simply labeled with this ID. Besides the assumption that there are n nodes that are generating voltage degrees of freedom, we assume that there are m links that generate degrees of freedom. Furthermore, referring to equation (34), we may rewrite (65) as

$$\mathbf{A}' * \mathbf{x} = \mathbf{b} \qquad \mathbf{x} = \begin{bmatrix} V_1 \\ \cdot \\ \cdot \\ V_n \\ A_1 \\ \cdot \\ \cdot \\ A_m \\ \Pi_1 \\ \cdot \\ \cdot \\ \Pi_m \end{bmatrix} \tag{66}$$

where $\mathbf{A}'$ represent the operator $\mathcal{G}$ of (34).

4.3 Discretization of the Maxwell-Ampere system

Just as for nodal variables, the entities associated to other geometrical objects, such as links or surfaces, we must first limit ourselves to a finite subset of links. Whereas Equation (26) is written down for the complete 'universe', a domain restriction is required. Suppose, we have a finite domain Ω selected. Furthermore, a grid is built using the nodes that were identified in the foregoing section. Next, we focus on all the links that connect these nodes. Again, some links will be found on the surface of Ω, to be precise, $(ij) \in \partial\Omega$. The construction of the equations of motion (and/or constrain equations) requires special care, because the finite-integration methods around such links we bring us outside Ω and that falls outside the region for which we compute information. We will first consider the situation when (ij) is an internal link, i.e. the link is not at the surface of the simulation domain.

Let us start with Equation (35) and consider for each link its dual surface. We will take the integral of this equation over the dual surface. Furthermore, we multiply the results with the length L of the link and obtain

$$\begin{aligned} \epsilon L \frac{\partial}{\partial t} \int_{\Delta S} \mathrm{d}\mathbf{S} \cdot \mathbf{\Pi} \quad &+ \quad L \int_{\Delta S} \mathrm{d}\mathbf{S} \cdot \nabla \times \left(\frac{1}{\mu} \nabla \times \mathbf{A} \right) - L \int_{\Delta S} \mathrm{d}\mathbf{S} \cdot \frac{1}{\mu} \nabla \left(\nabla \cdot \mathbf{A} \right) \\ + L \int_{\Delta S} \mathrm{d}\mathbf{S} \cdot \sigma \nabla V \quad &+ \quad L \int_{\Delta S} \mathrm{d}\mathbf{S} \cdot \sigma \mathbf{\Pi} \quad = \quad 0 \end{aligned} \tag{67}$$

Here, we put the equation in the appearance $lhs = 0$.

The discretization of each term will now be discussed. Starting at the left-hand side, we define a link variable Π_{ij} for the link going from node i to node j. The surface integral is approximated by taking $\mathbf{\Pi}$ constant over the dual area. Thus

$$\epsilon L \frac{\partial}{\partial t} \int_{\Delta S} \mathrm{d}\mathbf{S} \cdot \mathbf{\Pi} \simeq \epsilon L \, \Delta S_{ij} \, \frac{d\Pi_{ij}}{dt} \tag{68}$$

We can assign to each link a volume being $\Delta v_{ij} = L \, \Delta S_{ij}$. The second term on the right-hand side is dealt with using Stokes theorem twice in order to evaluate the circulations.

$$L \int_{\Delta S} \mathrm{d}\mathbf{S} \cdot \nabla \times \left(\frac{1}{\mu} \nabla \times \mathbf{A} \right) = L \oint_{\partial(\Delta S)} \mathrm{d}\mathbf{l} \cdot \left(\frac{1}{\mu} \nabla \times \mathbf{A} \right) \tag{69}$$

The circumference $\partial(\Delta S)$ consists of N segments. Each segment corresponds to a dual link that pierces through a *primary* surface. Therefore, we may approximate the right-hand side of (69) as

$$L \oint_{\partial(\Delta S)} \mathrm{d}\mathbf{l} \cdot \left(\frac{1}{\mu} \nabla \times \mathbf{A} \right) = L \sum_{k=1}^{N} \Delta l_k \, \frac{1}{\mu_k} \, \left(\nabla \times \mathbf{A} \right)_k \tag{70}$$

where the sum goes over all primary surfaces that were identified above as belonging to the circulation around the starting link. Note that we also attached an index on μ. This will guarantee that the correct value is taken depending in which material the segment Δl_k is located.

Next we must obtain an appropriate expression for $\left(\nabla \times \mathbf{A} \right)_k$. For that purpose, we consider the primary surfaces. In particular, an approximation for this expression is found by using

$$\left(\nabla \times \mathbf{A} \right)_k \simeq \frac{1}{\Delta S_k} \int_{\Delta S_k} \mathrm{d}\mathbf{S} \cdot \nabla \times \mathbf{A} = \frac{1}{\Delta S_k} \oint_{\partial(\Delta S_k)} \mathrm{d}\mathbf{l} \cdot \mathbf{A} \tag{71}$$

The last contour integral is evidently replaced by the collection of primary links variables around the primary surface. As a consequence, the second term at the right-hand side of (67) becomes

$$L \sum_{k=1}^{N} \Delta l_k \, \frac{1}{\mu_k} \, \frac{1}{\Delta S_k} \left(\sum_{l=1}^{N'} \Delta l_{<kl>} A_{<kl>} \right) \tag{72}$$

where we distinguished the link labeling from node labeling (ij) to surface labeling $< kl >$.

There is a subtlety related to the use of Equations (70) and (71). Note that we apply the value of magnetic induction that is evaluated at the center of the dual surface for all positions at the dual link. Our discretization picture is that once that we moved to discrete variables we may imagine these variables to be located at the nodes and at the links. For the currents this does mean that the discretized link currents are located at the links themselves. The computation

of the B-field contour integral around the dual surface can be corrected for the distance away from this link current. In (71) we use the maximum value of $|\mathbf{B}|$ along the link. This value can be corrected for the distance away from the primary link. This leads to a correction factor of

$$\alpha(\theta) = \left(\int_0^{\theta} \frac{\mathrm{d}\theta'}{cos\ \theta'} \right) / \left(\int_0^{\theta} \frac{\mathrm{d}\theta'}{cos^2\ \theta'} \right) \tag{73}$$

The function is shown in Fig. 4. The figure shows the inverse of $\alpha(\theta)$ how the correction factor depends on the acuteness of θ.

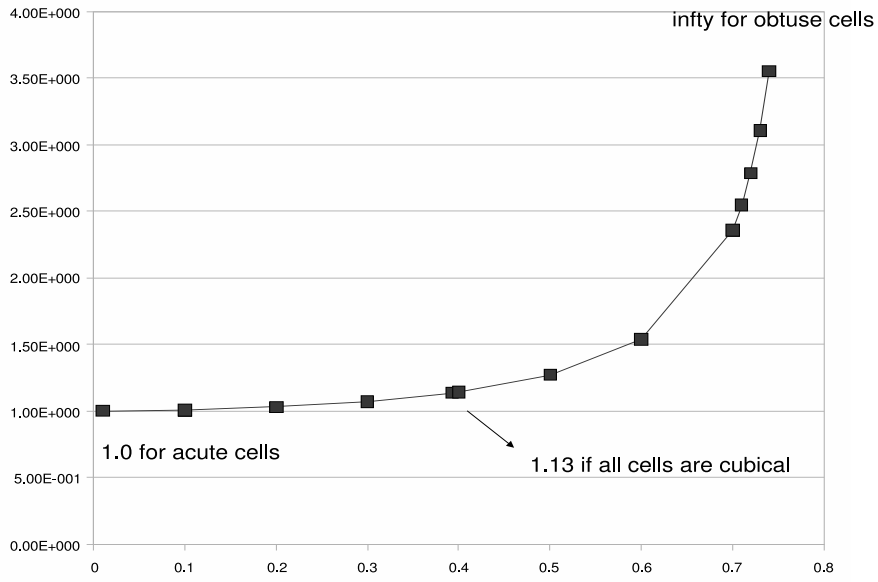

Figure 4: Correction factor as a function of the acuteness of the discretization cells.

For $\theta = \pi/4$ this gives $\alpha = 0.88$. Therefore, we will discretize the Maxwell-Ampere system by including this correction factor. It is possible to compute θ for each dual surface segment. However, this fine tuning is not further considered. So finally, we obtain

$$L \int_{\Delta S} \mathrm{d}\mathbf{S} \cdot \nabla \times \left(\frac{1}{\mu} \nabla \times \mathbf{A} \right) = L \sum_{k=1}^{N} \Delta l_k \, \frac{\alpha}{\mu_k} \, \frac{1}{\Delta S_k} \left(\sum_{l=1}^{N'} \Delta l_{<kl>} A_{<kl>} \right) \tag{74}$$

Next we consider the third term of (67). Now we use the fact that each link has a specific orientation from 'front' to 'back' (see section 5.4)

$$-L \int_{\Delta S} \mathrm{d}\mathbf{S} \cdot \frac{1}{\mu} \nabla \left(\nabla \cdot \mathbf{A} \right) \simeq - \int_{\Delta S} \mathrm{d}\mathbf{S} \cdot \frac{1}{\mu} \left(\nabla \cdot \mathbf{A} \right)_{back} + \int_{\Delta S} \mathrm{d}\mathbf{S} \cdot \frac{1}{\mu} \left(\nabla \cdot \mathbf{A} \right)_{front} \tag{75}$$

The link orientation coding is illustrated in Fig. 5.

The two term in (75) are now discretized as

$$\begin{aligned} \int_{\Delta S} \mathrm{d}\mathbf{S} \cdot \frac{1}{\mu} \left(\nabla \cdot \mathbf{A} \right) &= \frac{\Delta S}{\mu \Delta v} \int_{\Delta v} \mathrm{d}v \nabla \cdot \mathbf{A} \\ &= \frac{\Delta S}{\mu \Delta v} \oint_{\partial(\Delta v)} \mathrm{d}\mathbf{S} \cdot \mathbf{A} \\ &= \frac{\Delta S}{\mu \Delta v} \sum_{j}^{n} \Delta S_{ij} A_{ij} \end{aligned} \tag{76}$$

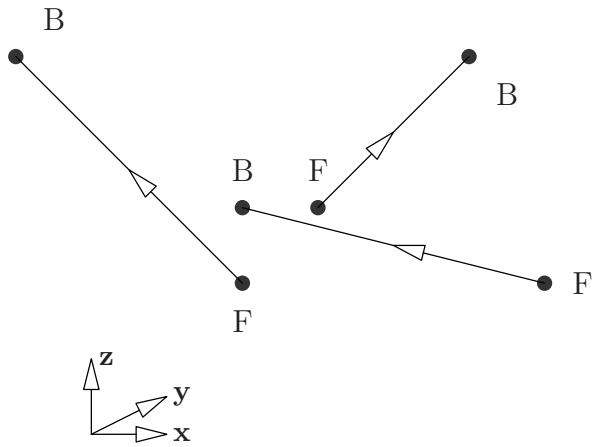

Figure 5: A collection of oriented links.

where the sum is now from the front or back node to their corresponding neighbor nodes. The boundary conditions enter this analysis in a specific way. Suppose the front or back node is on the surface of the simulation domain. Then the closed surface integral around such a node will require a dual area contribution from a dual area outside the simulation domain. These surfaces are by definition not considered.

However, we can go back to the gauge condition and use

$$\int_{\Delta S} \mathrm{d}\mathbf{S} \cdot \frac{1}{\mu} \left(\nabla \cdot \mathbf{A}\right) = -\Delta S \, \epsilon \frac{\partial V}{\partial t}. \tag{77}$$

At first sight this looks weird: First we insert the gauge condition to get rid of the singular character of the curl-curl operation and now we 'undo' this for nodes at the surface. This is however fine because for Dirichlet boundary conditions for $\mathbf{A}$ there are no closed circulations around primary surfaces and there there is no uniqueness problem and therefore the operator is well defined.

The last two terms are rather straightforward: For the fourth term we consider ∇V constant over the dual surface. Thus we obtain

$$L \int_{\Delta S} \mathrm{d}\mathbf{S} \cdot \sigma \nabla V = \left(V_{back} - V_{front}\right) \left(\sum \Delta S_i \sigma_i\right). \tag{78}$$

The variation of σ is taken into account by looking at each volume contribution separately.

The fourth term can be dealt with in a similar manner.

$$L \int_{\Delta S} \mathrm{d}\mathbf{S} \cdot \sigma \mathbf{\Pi} = L \, \Pi_{ij} \, \left(\sum \Delta S_i \sigma_i\right). \tag{79}$$

Collecting all terms, we come to the following structure for the discretized Maxwell-Ampere equation :

- Assuming Dirichlet's boundary conditions for the vector potential on the simulation domain boundary, we are dealing only with link degrees of freedom (DOF) corresponding to link that are inside the simulation domain.
- Assuming Neumann's boundary conditions, the links at the surface of the simulation domain also generate degrees of freedom.

- Each DOF-generating link induces two variables: A and Π, where $A = \mathbf{A}\cdot\mathbf{n}$ and $\Pi = \mathbf{\Pi}\cdot\mathbf{n}$ where $\mathbf{n}$ is the intrinsic link orientation,
- The Maxwell-Ampere equation is a time-evolution equation for $\mathbf{\Pi}$
- The time-evolution equation depends on V, A and Π as is summarized below.

$$\hat{\epsilon}\frac{\mathrm{d}}{\mathrm{d}t}\mathbf{\Pi} + M * \mathbf{V} + N * \mathbf{A} + \hat{\sigma} * \mathbf{\Pi} = 0 \qquad \mathbf{V} = \begin{bmatrix} V_1 \\ \cdot \\ \cdot \\ V_n \end{bmatrix} \qquad \mathbf{A} = \begin{bmatrix} A_1 \\ \cdot \\ \cdot \\ A_m \end{bmatrix} \qquad \mathbf{\Pi} = \begin{bmatrix} \Pi_1 \\ \cdot \\ \cdot \\ \Pi_m \end{bmatrix} \tag{80}$$

In here, $\hat{\epsilon}$ and $\hat{\sigma}$ are diagonal matrices that take care of the material and geometrical weighting of the permittivity and conductivity.

$$\hat{\epsilon} = \begin{bmatrix} \epsilon_1 & \cdot & \cdot & \cdot & \cdot \\ \cdot & \epsilon_2 \cdot & \cdot & \cdot & \\ \cdot & \cdot & \cdot & \cdot & \cdot \\ \cdot & \cdot & \cdot & \cdot & \cdot \\ \cdot & \cdot & \cdot & \cdot & \epsilon_m \end{bmatrix} \qquad \hat{\sigma} = \begin{bmatrix} \sigma_1 & \cdot & \cdot & \cdot & \cdot \\ \cdot & \sigma_2 \cdot & \cdot & \cdot & \\ \cdot & \cdot & \cdot & \cdot & \cdot \\ \cdot & \cdot & \cdot & \cdot & \cdot \\ \cdot & \cdot & \cdot & \cdot & \sigma_m \end{bmatrix} \tag{81}$$

The matrix N represents the discretization of the operator $\nabla \times [1/\mu \nabla \times \ ] - 1/\mu \nabla [\nabla \cdot \ ]$ as described above. The matrix N is of size $m \times m$. The matrix M describes the coupling to the voltage degrees of freedom and is of size $m \times n$.

Just as for Gauss' law, we can extract the matrices M, N, $\hat{\epsilon}$ and $\hat{\sigma}$ using the MAGWEL harmonic analysis solver.

4.4 Boundary conditions for the Maxwell-Ampere equation.

First of all, we emphasize that there are two classes of boundary conditions. We already mentioned that the vector potential consists of *three* components (fields) and each component requires its own boundary condition. Just for convenience, suppose we have a domain boundary parallel to the (x,y)-plane. The Dirichlet boundary conditions are that the x and y component of the vector potential are vanishing at the boundary, i.e. $A_x = 0$ and $A_y = 0$. We still have two more fields to consider : the potential V and the 3rd component A_z. At the surface we should also respect the gauge condition. In particular, in the Lorentz gauge, we obtain at the surface that

$$\frac{1}{\mu}\frac{\partial A_z}{\partial z} + \epsilon \frac{\partial V}{\partial t} = 0 \tag{82}$$

Since the the tangential components of A vanish at the surface, and therefore also their partial derivatives with respect to x and y. The Dirichlet boundary condition for A_x and A_y physically corresponds to a magnetic field arriving tangential at the surface. This field is described by the curl of the z-component of $\mathbf{A}$, i.e.

$$B_x = \frac{\partial A_z}{\partial x} \qquad B_y = -\frac{A_z}{\partial y} \qquad B_z = \frac{\partial A_y}{\partial x} - \frac{\partial A_x}{\partial y} = 0 \tag{83}$$

This is just the magnetic field corresponding the a current impinging perpendicular at the surface. Such a field is needed since we can not carry a current to a contact without also impinging

a magnetic field on that surface. So a good usage of the Dirichlet boundary condition is to use them for describing domain boundaries where contacts are found. Examples are pairs of contacts (ports) that are impinged by a TEM wave.

Contrary to Dirichlet boundary conditions, we also can imagine Neumann type of boundary conditions.

We look at a different class of boundary conditions for A_x and A_y. We will now invent something that resembles Neumann type boundary conditions for these fields. What could that be? Let us think of the surface parallel to the (x,y)-plane again. Now we want to say something about

$$\frac{\partial A_x}{\partial z} \qquad\qquad \frac{\partial A_y}{\partial z} \tag{84}$$

What can we say for these partial derivatives without using a primal link outside the simulation domain? Should we use links that by definition are not in the memory of the computer? No, we can say something about these partial derivatives. In Fig. 6 the red line outside the simulation domain is shown. When $\delta \to 0$ then one obtains above derivatives . So one obtains a component of the tangential magnetic field at the surface

$$\frac{\partial A_x}{\partial z} = -B_y = -\mathbf{B}\cdot\tau_y \qquad\qquad \frac{\partial A_y}{\partial z} = B_x = \mathbf{B}\cdot\tau_x \tag{85}$$

where τ is a tangential vector at the surface. For later use we define ν as a normal vector to the surface. So far, we did not achieve much. We substituted one piece of desired knowledge by another piece, since what to take for this $\mathbf{B}$? Here we may however apply some physics, Suppose that the boundary is located in some insulating region (air). Then we know that the solution satisfies the Maxwell equation in free space. Such solutions describe transverse polarized electromagnetic waves. *Asssuming* an outgoing wave perpendicular to the surface (in the z direction or in Fig. 6, in the direction of δ) , we can assert the value of these partial derivatives in terms of the link variables A_x and A_y themselves.

$$\mathbf{A}(\mathbf{x},t) = (A_x\mathbf{e}_x + A_y\mathbf{e}_y)\ \mathrm{e}^{j\omega t - jk_z z} \tag{86}$$

The plane TEM wave is characterized by a Dirichlet boundary condition on V, in particular $V=0$. Together with the gauge condition we find that $\mathbf{k}\cdot\mathbf{A}=0$, which explain (86). The wave satisfies

$$\left(\frac{1}{c^2}\frac{\partial^2}{\partial t^2} - \frac{\partial^2}{\partial z^2}\right)\mathbf{A} = 0 \tag{87}$$

In one dimension this is equivalent to

$$\left(\frac{1}{c}\frac{\partial}{\partial t} - \frac{\partial}{\partial z}\right)\left(\frac{1}{c}\frac{\partial}{\partial t} + \frac{\partial}{\partial z}\right)\mathbf{A} = 0 \tag{88}$$

For outgoing waves this boils down to

$$\left(\frac{1}{c}\frac{\partial}{\partial t} - \frac{\partial}{\partial z}\right)A_x = 0 \qquad\qquad \left(\frac{1}{c}\frac{\partial}{\partial t} - \frac{\partial}{\partial z}\right)A_y = 0 \tag{89}$$

This can be summarized as

$$\tau\cdot\mathbf{\Pi} = c\,(\nu\cdot\nabla)\tau\cdot\mathbf{A} \tag{90}$$

The Neumann boundary conditions for the surface links can be obtained from

$$\left(\frac{\partial}{\partial t} - c\,(\nu\cdot\nabla)\right)(\tau\cdot\mathbf{A}) = 0 \qquad\qquad \left(\frac{1}{c}\frac{\partial}{\partial t} - c\,(\nu\cdot\nabla)\right)(\tau\cdot\mathbf{\Pi}) = 0 \tag{91}$$

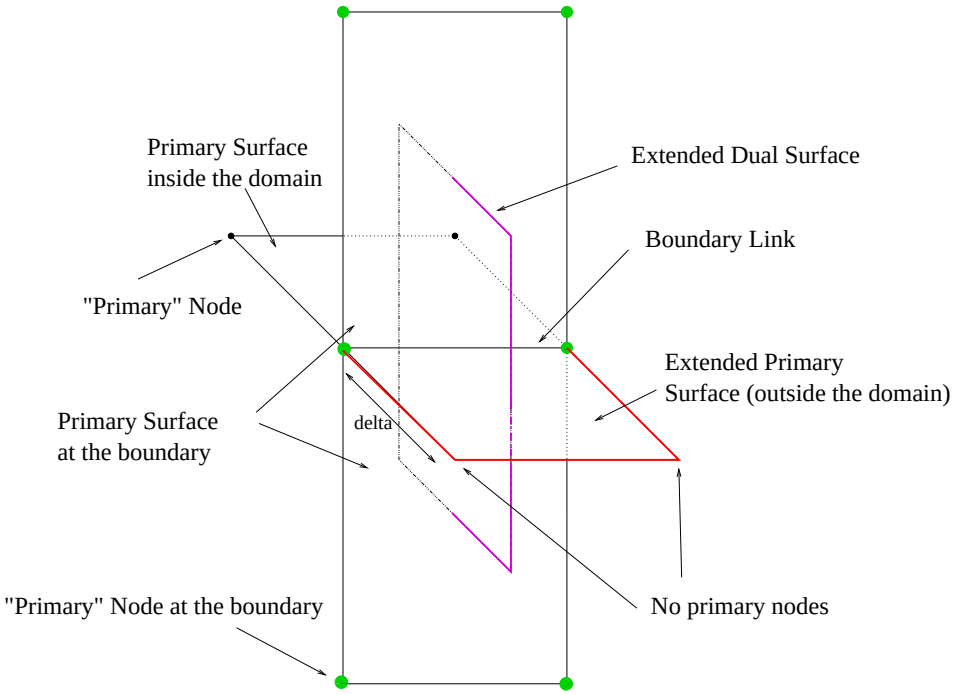

Figure 6: Sketch of the boundary nodes and links.

So far, we have specified the boundary condition for three fields : V, $\mathbf{A}\cdot\tau_x$ and $\mathbf{A}\cdot\tau_y$. Finally, we must discuss the normal component : $\mathbf{A}\cdot\nu$. Remember that for domain boundaries, where contacts are located we have give preference to the boundary conditions

- V Dirichlet type at contacts
- V Neumann type not at contact
- $\mathbf{A}_{//}$ Dirichlet type : $\mathbf{A}\cdot\tau_x = \mathbf{A}\cdot\tau_y = 0$
- $\mathbf{A}_{\perp}$ match of the gauge condition

The complementary set of boundary conditions will be applied only to domain boundaries where no contact areas are found. These boundaries will allow for incoming or outgoing EM radiation. From the the Maxwell-Ampere equation with $\mathbf{J}_{\text{cond}} = 0$ we obtain when *using* the gauge condition :

$$\left(\epsilon\,\frac{\partial^2}{\partial t^2} - \frac{1}{\mu}\nabla^2\right)(\mathbf{A}\cdot\nu) = 0 \tag{92}$$

The conditions read :

- V Dirichlet type at the domain boundary ($V = 0$)
- $\mathbf{A}_{//}$ Neumann type
- $\mathbf{A}_{\perp}$ match of the gauge condition, e.g. $\mathbf{A}_{\perp} = 0$

These conditions will likely to be fine for a very large domain such that a 'far-field' limit is valid. If the simulation domain is such that we have to enforce a truncation of the normal electric field then the following conditions apply :

- V Neumann type at the domain boundary : $(\nabla V) \cdot \nu = 0$
- $\mathbf{A}_{//}$ Neumann type
- $\mathbf{A}_{\perp}$ Dirichlet type, e.g. $\mathbf{A}_{\perp} = 0$

Note: Above description of the Neumann-type of boundary conditions can be seen as a first realization of the Mur boundary conditions that are applied for FDTD algorithms. In the latter case the underlying variables are the electric field $\mathbf{E}$ and $\mathbf{B}$. Here we applied the underlying ideas to the vector potential bfA. We have restricted ourselves to perpendicular changes with respect to the surface of the simulation domain. We also implemented the approach for waves arriving under a non-perpendicular angle to the surface, using Mur's idea of expanding the square-root operator in terms of a power series. However, numerical experiments showed a serious convergence flaw.

4.5 Generalized boundary conditions for the Maxwell-Ampere equation

When discussing Gauss' law we have discussed the two options for closing the equation at the surface of the simulation domain. At the surface either we applied Neumann boundary conditions if no contacts are present or Dirichlet boundary conditions. These two cases are not exhaustive and when discussing devices in interaction we must allow for various generalizations. First of all, although from a mathematical point of view it is convenient to think of boundary condition as belonging to the boundary of the simulation domain, from an engineering point of view the boundary conditions can be imposed at surface elements located *inside* the simulation domain. Whereas such a perception of boundary conditions for so-called internal contacts is can be imagined for Dirichlet boundary conditions one should realize that the internal contacts can also be used for current boundary conditions. In the latter case, the terminal currents are used to complete the system of equation leading to a well-defined problem. This is nicely illustrated in Fig. 7

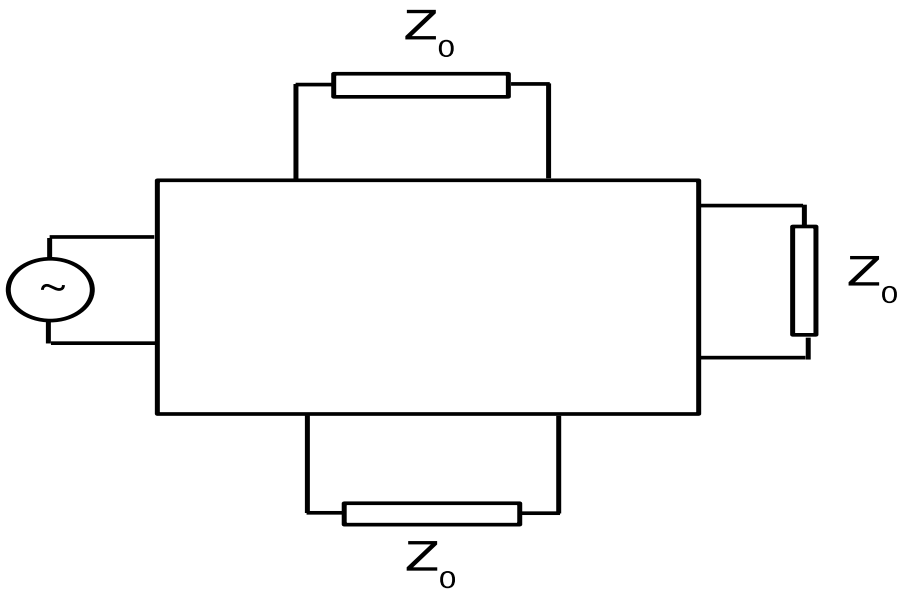

Figure 7: Set up for direct simulation of S-parameters.

In this set-up, the contacts are grouped in pairs. In order to extract one column of the S-matrix, one pair of contacts, i.e. ”port”, is excited with a frequency voltage signal, whereas all other ports (pair of contacts) are closed with a reference impedance, Z_0.

In order to evaluate the scattering matrix, say of an N-port system, we iterate over all ports and put a voltage difference over one port and put an impedance load over all other ports. Thus the potential variables of the contacts belonging to all but one port, become degrees of freedom that need to be evaluated. The following variable are required to understand the scattering matrices, where Z_0 is a real impedance that is usual taken to be 50 Ohms.

$$a_i = \frac{V_i + Z_0 I_i}{2\sqrt{Z_0}} \tag{93}$$

$$b_i = \frac{V_i - Z_0 I_i}{2\sqrt{Z_0}} \tag{94}$$

The variables a_i represent the voltage waves incident on the ports labeled with index i and the variables b_i represent the reflected voltages at ports i. The scattering parameters s_{ij} describe the relationship between the incident and reflected waves.

$$b_i = \sum_{j=1}^{N} s_{ij} a_j \tag{95}$$

The scattering matrix element s_{ij} can be found by putting a voltage signal on port i and place an impedance of Z_0 over all other ports. Then a_j is *z*ero by construction, since for those ports we have that $V_j = -Z_0 I_j$ and therefore,

$$s_{ij} = \frac{b_i}{a_j} \tag{96}$$

Note that the simulation set up extracts at each port the complex currents and voltages. Moreover, these values are assigned to contacts. Finally these contacts can very well be internal. Thus this modeling approach is ignores the presence of currents in the simulation domain once that they have been captured by the ports. How can that be made physically understood? The paradox is eliminated by considering in more detail how the ports are attached to the measurement equipment. The reference impedance represents the impedance of the coax wire of the measurement equipment. The simulation domain is restricted to the device environment volume *m*inus the volume occupied by the coax wires. Finally, we may consider idealized (infinitely thin) wires such that the full volume may be considered. The ports are connected to the measurement equipment with a string as a variation of a ”Dirac string” being an infinitely-thin coax wire. This idealization leads to a simulation domain of which the probe wires occupy an infinitesimal amount of space, which is neglected in setting up the domain. The results are internal contacts. This is illustrated in Fig. 8.

4.6 Discretization of the gauge condition

The Maxwell-Ampere equation is discretized with use of the gauge condition. Therefore, we better make sure that the gauge condition is really satisfied. In steady-state or in AC small-signal analysis, this was achieved implicitly by solving the current-continuity equations and Gauss' law, which were solved explicitly. In the set up of the transient simulation flow, we arrived at a different picture. To summarize:

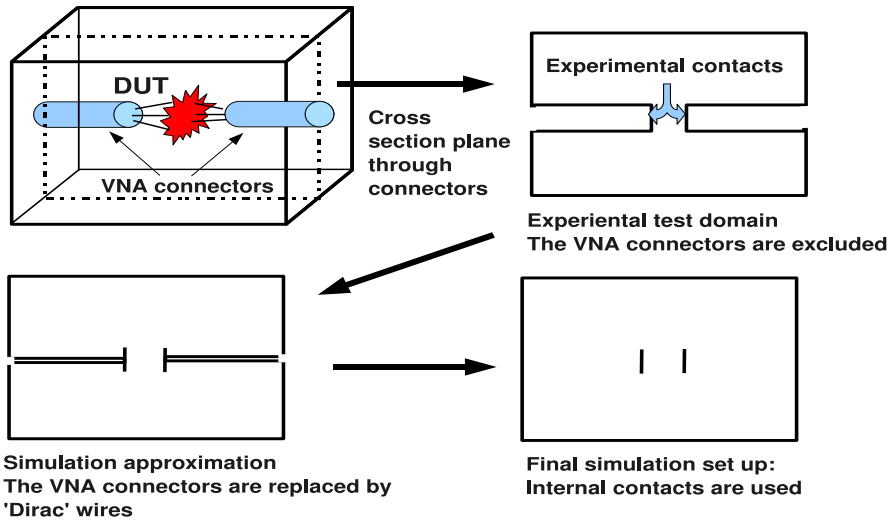

Figure 8: Illustration of the justification for using internal contacts.

- Solve the gauge condition explicitly : $\frac{1}{\mu}\nabla \cdot \mathbf{A} + \epsilon\frac{\partial V}{\partial t} = 0$
- Apply the validity of the gauge condition when discretizing the Maxwell-Ampere (MA) equations (see 26) : $\epsilon\frac{\partial \mathbf{\Pi}}{\partial t} + \nabla \times \left(\frac{1}{\mu}\nabla \times \mathbf{A}\right) - \frac{1}{\mu}\nabla\left(\nabla \cdot \mathbf{A}\right) + \sigma\nabla V + \sigma\mathbf{\Pi} = 0$
- Solve the current continuity equations : $\nabla \cdot \mathbf{J} + \frac{\partial \rho}{\partial t} = 0$
- Then Gauss' law is *implicitly satisfied* in the following way : $\frac{\partial \rho}{\partial t} = \frac{\partial}{\partial t}\left(\nabla \cdot \mathbf{D}\right)$
  Therefore, if Gauss' law is satisfied at $t = 0$, it will also be at $t > 0$. ([4])

This summary suggests that an alternative approach may be possible. We will start from Gauss' law and solve it explicitly at every time instance. This gives us the value of the charge density. The current-continuity equations are not regarded as a by product of the MA equation, but are considered as an independent set of equation to be solved, together with the MA equations. Then we arrive at the following scheme :

- Solve Gauss' law at each time step : $\rho + \nabla \cdot \left(\epsilon\left[\nabla V + \Pi\right]\right) = 0$
- Solve the current-continuity equation : $\frac{\partial \rho}{\partial t} - \nabla \cdot \left(\sigma\left[\nabla V + \Pi\right]\right) = 0$
- Solve the Maxwell-Ampere equation (as before).
- Then the gauge condition is *implicitly satisfied* as can be easily demonstrated by contracting the MA equation with the divergence operator and using the other two equations.

Both schemes are equivalent, but the second scheme is more difficult to implement if we want to express every variable in terms of ρ , $\mathbf{A}$ and $\mathbf{\Pi}$, i.e. eliminating V in favor of ρ, which can be

[4]This is the reason why we emphasized that the illustration of the discretization method using Gauss' law was primarily done for didactic reasons. In the transient simulator, Gauss' law is not explicitly solved.

done by the variable transformation :

$$\rho = \nabla \cdot \mathbf{D} \quad \Rightarrow V \; = - \int \mathrm{d}\mathbf{r} \;\; \nabla^{-2} \left(\frac{\rho}{\epsilon} + \nabla \cdot \mathbf{\Pi} \right) \tag{97}$$

For the time being, we will not further pursue the second scheme, because of the non-local nature of the variable transformation.

5 Temporal discretization

There exists several views to address above system of equations in the temporal regime. We can distinguish between the linear case (no semiconductors present) and the non-linear case (semiconductors included). In the latter case it is not useful to isolate the time differentiations from the equations. Therefore, we write the system of equations as a differential-algebraic equation (DAE) :

$$M * \frac{\mathrm{d}}{\mathrm{d}t}\mathbf{X}(t) + H(\mathbf{X}(t), t) + F * \mathbf{X}_{bc}(t) = 0 \tag{98a}$$

$$G(\mathbf{X}) = 0 \tag{98b}$$

Here, $\mathbf{G}$ is determined by the Gauss' equation. The other equations are collected in $(99\mathrm{a})$. $\mathbf{X}$ is the vector of unknowns $(V, \mathbf{A}, \mathbf{\Pi}, n, p)$ and $\mathbf{X}_{bc}(t)$ is the vector of boundary-condition values, which are coupled into the system via the operator F. We assumed that the boundary condition can be linked into the system using a linear operator. This is definitely the case for linear materials (insulators and metals) but this assumption must be revised for semi-conductors.

The discretized Maxwell equations for conductor / insulator systems lead to a linear system

$$M * \frac{\mathrm{d}}{\mathrm{d}t}\mathbf{X}(t) + H * \mathbf{X}(t) + F * \mathbf{X}_{bc}(t) = 0 \tag{99a}$$

$$G(\mathbf{X}) = 0 \tag{99b}$$

This DAE will be coupled to the MNA-equations (1) that describe the circuit's behavior. This coupling is given in two ways: on one hand, the currents at the contacts of the elements described by Maxwell-equations are added to the Kirchoff's current law equation in the network equations, and on the other hand, the boundary conditions for these elements depend on the node potentials of the circuit. The coupled system could have the following form

$$E * \frac{\mathrm{d}}{\mathrm{d}t} d(\mathbf{Y}, t) + b(\mathbf{Y}, t) + c(\mathbf{Y}_{ext}, t) = 0, \tag{100a}$$

$$g(\mathbf{X}, \mathbf{Y}, \frac{\mathrm{d}}{\mathrm{d}t}\mathbf{X}, t) = 0 \tag{100b}$$

$$M * \frac{\mathrm{d}}{\mathrm{d}t}\mathbf{X} + H(\mathbf{X}, t) + F * \mathbf{Y} = 0, \tag{100c}$$

$$\mathbf{G}(\mathbf{X}, \mathbf{Y}) = 0. \tag{100d}$$

with $\mathbf{Y} = (e, j_L, j_V, j_M)$ being the network variables: all node potentials e, the currents j_L through inductances, the currents j_V through voltages sources and the currents j_M through the EM elements. Note that the list $includes$ all currents entering and leaving the EM elements. As argued before, each contact of the EM element induces a current variable j_M^i.

Equation $(100\mathrm{a})$ describes the circuit equations. We did put the external current and voltage sources into a separate function $c(Y_{ext}, t)$. These variables are the true external boundary

conditions of the coupled system contrary to the variables j_M^i that are contributing to the set of unknowns.

The equations $(100\mathrm{c})$ and $(100\mathrm{d})$ describe the Maxwell equations corresponding to the field-solver (FS) problem. Here, we made the important assertion that (a sub set) of the MNA variables act as boundary-condition variables, i.e. $\mathbf{X}_{bc}(t) \subset \mathbf{Y}(t)$ The coupling between both is given by $(100\mathrm{b})$. In more detail, equation system $(100\mathrm{a})$ has the form

$$A_C \frac{\mathrm{d}}{\mathrm{d}t} q_C(A_C^\mathsf{T} e, t) + A_R g_R(A_R^\mathsf{T} e, t) + A_L j_L + A_V j_V + A_M j_M + A_I i_s(t) = 0, \tag{101}$$

$$\frac{\mathrm{d}}{\mathrm{d}t} \phi(j_L, t) - A_L^\mathsf{T} e = 0, \tag{102}$$

$$A_V^\mathsf{T} e - v_s(t) = 0. \tag{103}$$

The coupling equations $(100\mathrm{b})$ look like

$$g_{\mathrm{FS}\to\mathrm{MNA}}(A_M^\mathsf{T} e, j_M, \mathbf{X}, \frac{\mathrm{d}}{\mathrm{d}t}\mathbf{X}) = 0 \tag{104}$$

The applied potential at the EM elements is given by $A_M^\mathsf{T} e$, which constitute a subset of the variables $\mathbf{Y}$.

Furthermore , there exists a second coupling that informs us how the MNA system inpacts the solutions from the field solver. In a first approach, we will use Dirichlet's boundary conditions. This implies that the applied voltages at the contacts are the linked to the field-solver degrees of freedom as the contact voltages

$$g_{\mathrm{MNA}\to\mathrm{FS}}(A_M^\mathsf{T} e, \mathbf{X}) = 0 \tag{105}$$

This coupling is already accounted for by the third term in 100c.

In order to gain a more pictorial understanding of the coupled problem, we consider the combined vector $\mathbf{Z}$ of $\mathbf{X}$ and $\mathbf{Y}$.

$$\mathbf{Z} = \begin{bmatrix} \mathbf{X} \\ \mathbf{Y} \end{bmatrix} \tag{106}$$

In this vector, $\mathbf{X} = \{V_1, V_2, ..., A_1, A_2 ..., \Pi_1, \Pi_2, ..., p_1, p_2, ..., n_1, n_2 ...\}$ represents all field degrees of freedom and $\mathbf{Y} = \{e_1, e_2, ..., j_1, j_2, , , , , , j_M^1, j_M^2, ...\}$ represents all MNA variables as identified above.

The integrated circuit-field-solver will address the following equation :

$$\frac{\mathrm{d}}{\mathrm{d}t}\mathcal{U}(\mathbf{Z}, t) + \mathcal{V}(\mathbf{Z}, t) + \mathcal{W}(\mathbf{Z}_{ext}) = 0 \tag{107}$$

$$\mathcal{U} = \begin{bmatrix} \mathcal{U}_{11} & \mathcal{U}_{12} \\ \mathcal{U}_{21} & \mathcal{U}_{22} \end{bmatrix} \qquad \mathcal{V} = \begin{bmatrix} \mathcal{V}_{11} & \mathcal{V}_{12} \\ \mathcal{V}_{21} & \mathcal{V}_{22} \end{bmatrix} \qquad \mathcal{W} = \begin{bmatrix} \mathcal{W}_{11} & \mathcal{W}_{12} \\ \mathcal{W}_{21} & \mathcal{W}_{22} \end{bmatrix} \tag{108}$$

The entries of the $\mathcal{U}, \mathcal{V}$ and $\mathcal{W}$ are all functions of $\mathbf{Z}$ and t. At this stage, we would like to introduce a new notation. Whereas a matrix-vector multiplication by default refers to a linear operation, we are in need for allowing non-linear functions in given parts of the assemble of matrices.

Consider a collection of functions $\{F_{ij} | i = 1, ...n, j = 1, ...m\}$. The ij-th function has as input a vector $\mathbf{X}_j$ with dimension D_j and generates an output vector $\mathbf{Y}_i$ of dimension D_i. Thus

$$\mathbf{Y}_i = F_{ij}(\mathbf{X}_j) \tag{109}$$

The namings $\mathbf{X}$ and $\mathbf{Y}$ are *not* referring to the previous use of these vector names! The collection of functions can be grouped in a matrix.

$$\begin{bmatrix} \mathbf{Y}_1 \\ \mathbf{Y}_2 \\ \vdots \\ \mathbf{Y}_n \end{bmatrix} = \begin{bmatrix} F_{11}(\mathbf{X}_1) & F_{12}(\mathbf{X}_2) & \cdots & F_{1m}(\mathbf{X}_m) \\ F_{21}(\mathbf{X}_1) & F_{12}(\mathbf{X}_2) & \cdots & F_{1m}(\mathbf{X}_m) \\ \vdots & \vdots & & \vdots \\ F_{n1}(\mathbf{X}_1) & F_{n2}(\mathbf{X}_2) & \cdots & F_{nm}(\mathbf{X}_m) \end{bmatrix} \tag{110}$$

We will now use an underlining of the indices if the function is non-linear.

Definition:

$$F_{\underline{ij}} * \mathbf{X}_j = F_{ij}(\mathbf{X}_j) \qquad \text{for a non-linear function.} \tag{111}$$

Using this notation equation (107) becomes (now $\mathbf{X}$ and $\mathbf{Y}$ refer the field variables and MNA variables)

$$\frac{\mathrm{d}}{\mathrm{d}t} \begin{bmatrix} \mathcal{U}_{11} & \mathbf{0} \\ \mathbf{0} & \mathcal{U}_{\underline{22}}(t) \end{bmatrix} * \begin{bmatrix} \mathbf{X} \\ \mathbf{Y} \end{bmatrix} + \begin{bmatrix} \mathcal{V}_{\underline{11}} & \mathcal{V}_{12} \\ \mathcal{V}_{21} & \mathcal{V}_{\underline{22}} \end{bmatrix} * \begin{bmatrix} \mathbf{X} \\ \mathbf{Y} \end{bmatrix} + \begin{bmatrix} \mathbf{0} & \mathbf{0} \\ \mathbf{0} & \mathcal{W}_{\underline{22}} \end{bmatrix} * \begin{bmatrix} \mathbf{0} \\ \mathbf{Y}_{ext} \end{bmatrix} = 0 \tag{112}$$

The entries in (112) were written down earlier as

$$\frac{\mathrm{d}}{\mathrm{d}t} \begin{bmatrix} M & \mathbf{0} \\ \mathbf{0} & E \,.\, d \end{bmatrix} * \begin{bmatrix} \mathbf{X} \\ \mathbf{Y} \end{bmatrix} + \begin{bmatrix} H & F \\ g_{\mathrm{FS}\to\mathrm{MNA}} & b(t) \end{bmatrix} * \begin{bmatrix} \mathbf{X} \\ \mathbf{Y} \end{bmatrix} + \begin{bmatrix} \mathbf{0} & \mathbf{0} \\ \mathbf{0} & c \end{bmatrix} * \begin{bmatrix} \mathbf{0} \\ \mathbf{Y}_{ext} \end{bmatrix} = 0 \tag{113}$$

5.1 How does the functions $g_{FS\to MNA}$ looks like?

In order to answer the question, we will consider a simple example and attempt to submit it to a combined circuit/field solving procedure. As a starting point we will will consider a simple one-winding prototype inductor and attach a small circuit to it. The inductor has two contacts (it is not considered as a multiple-port system but as a EM element that requires voltages as input and gives a current response. There are two contacts (one is visible as a red plate) to which we can attach a circuit. In the next section we will consider the equation construction in detail. The coupling that we want to describe is the between a contact current, j_M, a contact voltage e and a set of field degrees of freedom $\mathbf{X}$. Current continuity at the contact plane provides a connection between these variables. This is illustrated in Fig. 9.

The sum of the current into the contact plane must be adding up to zero. From the ”inside” , i.e. from the field solvers perspective a collection of currents arrives at the contact plane. This current is a sum of all contributions from the links attached to the contact. Each link contributes the current $J_{ij}^{\mathrm{cond}} + J_{ij}^{\mathrm{displ}}$. Since the displacement current also contributes to the current, we obtain that the ”inside” current is

$$I_{\mathrm{inside}} = \sum_k w_k^1 \left(e_{\mathrm{contact}} - V_k\right) + \sum_l \left(w_l^2 \; A_l + w_l^3 \; \Pi_l\right) \tag{114}$$

where the factor w^i are determined by material parameters ϵ and σ and geometrical details and the sums go over the nodes and links that connected to the nodes of the contact planes.

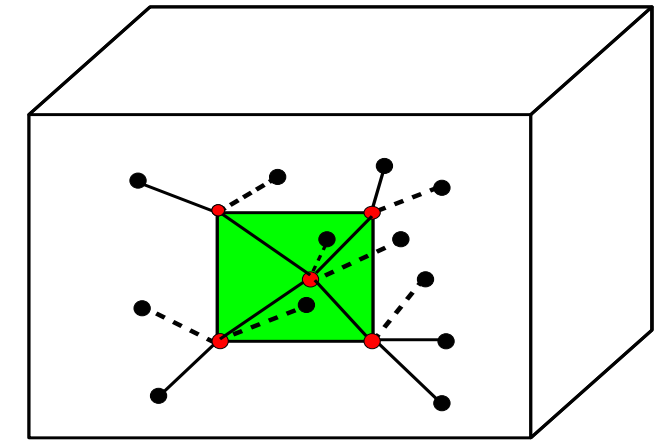

Contact plane (green) with contact nodes and connected nodes (black)
All the links to the contact nodes are also shown.

Figure 9: Illustration of the contact nodes and links participating in the coupling.

From the MNA perspective we deal with a current variable j_M. The function g just expresses the continuity of the current

$$j_M + I_{\text{inside}} = 0 \tag{115}$$

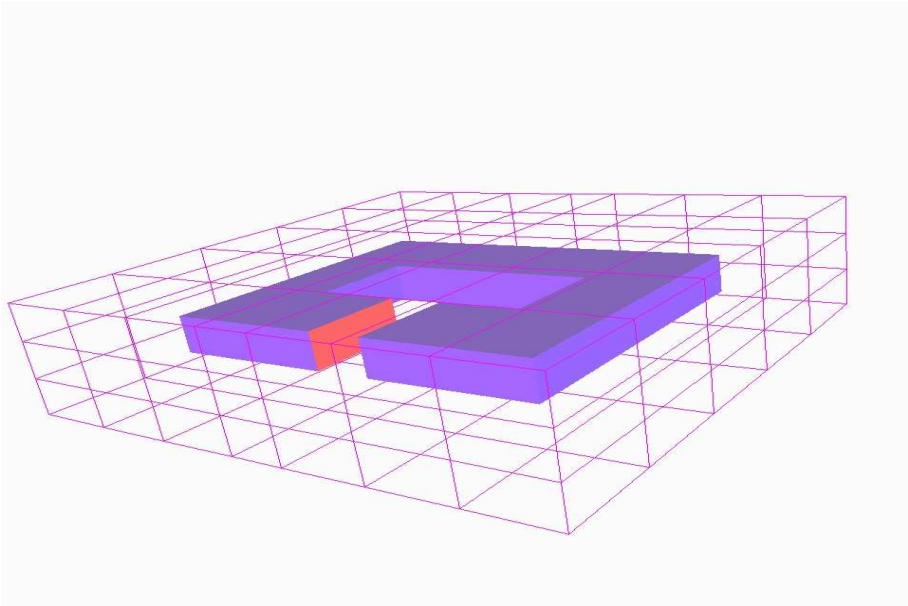

Figure 10: Prototype inductor with mesh.

5.2 An MNA approach for setting up the coupled system

The foregoing section was clearly composed starting from a field-solver 'language' and adding MNA equations to it. Of course there is no superiority in this approach. One can just as well

start from an MNA perspective and add the field equation. This will be done in this section. Note that we list the variable : first MNA and next FS.

In order to treat the whole coupled system (100) by time integration, we rewrite it as a DAE with the following structure

$$A\frac{\mathrm{d}}{\mathrm{d}t}d(Y,t)+b(Y,t)=0, \tag{116}$$

where Y is the vector of unknowns $Y=(e,j_L,j_V,j_M,X)$. The matrix A is usually a singular but constant matrix. As shown in the DAE should have a properly stated term in order to avoid time stepsize reductions because of certain stability problems. It means, we should formulate A and d such that

$$\ker A \cap \operatorname{im} D = \{0\}.$$

with $D(Y,t) := \partial_Y d(Y,t)$.

For example, the DAE (1) can be written as a DAE with the form (116) with

$$A=\begin{pmatrix} A_C & 0 \\ 0 & I \\ 0 & 0 \end{pmatrix}, \qquad d(e,j_L,j_V)=\begin{pmatrix} q_C(A_C^{\mathsf{T}}e,t) \\ \phi(j_L,t) \end{pmatrix},$$

and

$$b(e,j_L,j_V)=\begin{pmatrix} A_R g_R(A_R^{\mathsf{T}}e,t)+A_L j_L+A_V j_V+A_I i_s(t) \\ -A_L^{\mathsf{T}}e \\ A_V^{\mathsf{T}}e-v_s(t) \end{pmatrix}.$$

The coupled system (100) can be written as (116) with

$$A=\begin{pmatrix} A_C & 0 & 0 & 0 \\ 0 & I & 0 & 0 \\ 0 & 0 & 0 & 0 \\ 0 & 0 & I & 0 \\ 0 & 0 & 0 & \mathbf{M} \\ 0 & 0 & 0 & 0 \end{pmatrix}, \qquad d=\begin{pmatrix} q_C(A_C^{\mathsf{T}}e,t) \\ \phi(j_L,t) \\ q_M(\mathbf{X},A_M^{\mathsf{T}}e,t) \\ \mathbf{X} \end{pmatrix},$$

and

$$b=\begin{pmatrix} A_R g_R(A_R^{\mathsf{T}}e,t)+A_L j_L+A_V j_V+A_M j_M+A_I i_s(t) \\ -A_L^{\mathsf{T}}e \\ A_V^{\mathsf{T}}e-v_s(t) \\ g_M(A_M^{\mathsf{T}}e,j_M,\mathbf{X},t) \\ \mathbf{H}(t,\mathbf{X},A_M^{\mathsf{T}}e,j_M) \\ \mathbf{G}(\mathbf{X},A_M^{\mathsf{T}}e,j_M) \end{pmatrix}.$$

For the transient simulation of DAEs (116), we need an implicit time integration. The first method of choice are the Backward Differentiation Formulas (BDF). They do not produce discretization errors in the algebraic equations. Furthermore, one can get higher order of convergence without enlarging the system of equations. Note, the implicit Euler method is a special case of BDF having order 1.

5.2.1 BDF for DAEs

First, we explain the standard way of using k-step BDF methods when integrating DAEs in standard form

$$f(x',x,t)=0, \quad t\in[t_0,t_F].$$

Suppose that the approximations $x_{n-j} \approx x(t_{n-j}),\ j = 1, 2, \ldots, k$ have already been calculated. We denote $\tau_m = t_m - t_{m-1},\ m = 1, 2, \ldots$ as the m-th time step. An approximation x_n to $x(t_n)$ will be obtained by solving the nonlinear equation

$$f\left(\frac{1}{\tau_n}\sum_{j=0}^{k}\alpha_{j,n}x_{n-j}, x_n, t_n\right) = 0.$$

The BDF coefficients $\alpha_{0,n}, \alpha_{1,n}, \ldots, \alpha_{k,n}$ depend on the stepsizes $\tau_n, \tau_{n-1}, \ldots, \tau_{n-k+1}$ (if the time stepsize is not constant). They are determined such that the derivative $x'(t_n)$ is approximated by

$$x'(t_n) \approx \frac{1}{\tau_n}\sum_{j=0}^{k}\alpha_{j,n}x_{n-j}.$$

with order k. In case of index-1 DAEs, the order of convergence of the BDF method equals k. In case of index-2 DAEs, one may lose one order of τ. In case of index-3 DAEs, the BDF method may fail completely. Therefore, we should check whether our coupled system has at most index 2 as the circuit equations have.

In order to obtain an approximation Y_n to the value of $Y(t_n)$, where $Y(t)$ is the exact solution of (116), we proceed in a similar way. In this case, the derivative $d'(Y(t_n), t_n)$ is replaced by a sum approximating it, Y_n is then the solution of the nonlinear equation

$$A\left(\frac{1}{\tau_n}\sum_{j=0}^{k}\alpha_{j,n}d\left(Y_{n-j}, t_{n-j}\right)\right) + b(Y_n, t_n) = 0.$$

If e.g. the MNA equations are solved with BDF methods, the approximations $e_n, j_{L,n}$ and $j_{V,n}$ to $e(t_n), j_L(t_n), j_V(t_n),\ n = 1, 2, \ldots$ are the solution of the nonlinear system of equations

$$\begin{aligned} A_C\frac{1}{\tau_n}\left(\sum_{j=0}^{k}\alpha_{j,n}q_C(A_C^{\mathsf{T}}e_{n-j}, t_{n-j})\right) + A_R g_R(A_R^{\mathsf{T}}e_n, t_n) + A_L j_{L,n} + A_V j_{V,n} + A_I i_s(t_n) &= 0, \\ \frac{1}{\tau_n}\left(\sum_{j=0}^{k}\alpha_{j,n}\phi(j_{L,n-j}, t_{n-j})\right) - A_L^{\mathsf{T}}e_n &= 0, \\ A_V^{\mathsf{T}}e_n - v_s(t_n) &= 0. \end{aligned}$$

In the special case of the implicit Euler method we have $k = 1$, $\alpha_{0,n} = 1, \alpha_{1,n} = 1$. The values $e_n, j_{L,n}$ and $j_{V,n}$ are then obtained by solving the following system of equations

$$\begin{aligned} A_C\frac{1}{\tau_n}\Big(q_C(A_C^{\mathsf{T}}e_n, t_n) - q_C(A_C^{\mathsf{T}}e_{n-1}, t_{n-1})\Big) + A_R g_R(A_R^{\mathsf{T}}e_n, t_n) + A_L j_{L,n} + A_V j_{V,n} + A_I i_s(t_n) &= 0, \\ \frac{1}{\tau_n}\left(\phi(j_{L,n}, t_n) - \phi(j_{L,n-1}, t_{n-1})\right) - A_L^{\mathsf{T}}e_n &= 0, \\ A_V^{\mathsf{T}}e_n - v_s(t_n) &= 0. \end{aligned}$$

5.2.2 Coupled system MNA+discretized Drift-Diffusion equations

Suppose the Drift-Diffusion (DD) equations for describing the semiconductor devices in an electrical circuit are discretized in space with e.g., the Scharfetter-Gummel discretization method.

The DAE associated to the coupled system of discretized Drift-Diffusion equations and MNA equations has the general form

$$A_C \frac{\mathrm{d}}{\mathrm{d}t} q_C(A_C^\mathsf{T} e, t) + A_R g_R(A_R^\mathsf{T} e, t) + A_L j_L + A_V j_V + A_S j_S + A_I i_s(t) = 0, \tag{117a}$$

$$\frac{\mathrm{d}}{\mathrm{d}t} \phi(j_L, t) - A_L^\mathsf{T} e = 0, \tag{117b}$$

$$A_V^\mathsf{T} e - v_s(t) = 0, \tag{117c}$$

$$j_S + g_S(A_S^\mathsf{T} e, \Psi, N, P) + \frac{\mathrm{d}}{\mathrm{d}t} q_S(\Psi, A_S^\mathsf{T} e, t) = 0, \tag{117d}$$

$$T\Psi + D(C - N + P) = 0, \tag{117e}$$

$$DN' + j_N(A_S^\mathsf{T} e, \Psi, N) + R(N, P) = 0, \tag{117f}$$

$$DP' - j_P(A_S^\mathsf{T} e, \Psi, P) + R(N, P) = 0. \tag{117g}$$

The matrix A_S is an incidence matrix, j_S denotes the currents at the semiconductor's contacts. The potentials applied at the semiconductor's contacts depend on $A_S^\mathsf{T} e$ (that's why (117d)-(117g) depend on it). The matrices T and D are non-singular and constant in time. They depend on the spatial mesh. $\Psi(t), N(t)$ and $P(t)$ are for each t approximations to the values of the electrostatic potential and the electrons and holes densities respectively on the mesh points. Equation (117e) is the discretized Poisson-equation, while (117f)-(117g) are the discretized continuity equations for the electrons and holes densities. In equation (117d) the current at the semiconductor's contacts is calculated, it is the sum of the current caused by electrons and holes $g_S(A_S^\mathsf{T} e, \Psi, N, P)$ and the displacement current $\frac{\mathrm{d}}{\mathrm{d}t} q_S(\Psi, A_S^\mathsf{T} e, t)$. This DAE can be written as a DAE with properly stated leading term with

$$A = \begin{pmatrix} A_C & 0 & 0 & 0 & 0 \\ 0 & I & 0 & 0 & 0 \\ 0 & 0 & 0 & 0 & 0 \\ 0 & 0 & I & 0 & 0 \\ 0 & 0 & 0 & 0 & 0 \\ 0 & 0 & 0 & I & 0 \\ 0 & 0 & 0 & 0 & I \end{pmatrix}, \quad d = \begin{pmatrix} q_C(A_C^\mathsf{T} e, t) \\ \phi(j_L, t) \\ q_S(\Psi, A_S^\mathsf{T} e, t) \\ DN \\ DP \end{pmatrix}$$

and

$$b = \begin{pmatrix} A_R g_R(A_R^\mathsf{T} e, t) + A_L j_L + A_V j_V + A_S j_S + A_I i_s(t) \\ -A_L^\mathsf{T} e \\ A_V^\mathsf{T} e - v_s(t) \\ j_S + g_S(A_S^\mathsf{T} e, \Psi, N, P) \\ T\Psi + D(C - N + P) \\ j_N(A_S^\mathsf{T} e, \Psi, N) + R(N, P) \\ -j_P(A_S^\mathsf{T} e, \Psi, P) + R(N, P) \end{pmatrix}$$

The index of this DAE is always less or equal to two. If it is solved with the k-steps BDF method, approximations $e_n, j_{L,n}, j_{V,n}, j_{S,n}, \Psi_n, N_n$ and P_n to $e(t_n), j_L(t_n), j_V(t_n), j_S(t_n), \Psi(t_n), N(t_n)$ and

$P(t_n)$ are obtained by solving the following system of nonlinear equations

$$A_C \frac{1}{\tau_n} \left(\sum_{j=0}^{k} \alpha_{j,n} q_C(A_C^\mathsf{T} e_{n-j}, t_{n-j}) \right) + A_R g_R(A_R^\mathsf{T} e_n, t_n) + A_L j_{L,n} + A_V j_{V,n} + A_S j_{S,n} + A_I i_s(t_n) = 0,$$

$$\frac{1}{\tau_n} \left(\sum_{j=0}^{k} \alpha_{j,n} \phi(j_{L,n-j}, t_{n-j}) \right) - A_L^\mathsf{T} e_n = 0,$$

$$A_V^\mathsf{T} e_n - v_s(t_n) = 0,$$

$$j_{S,n} + g_S(A_S^\mathsf{T} e_n, \Psi_n, N_n, P_n) + \frac{1}{\tau_n} \sum_{j=0}^{k} \alpha_{j,n} q_S(\Psi_{n-j}, A_S^\mathsf{T} e_{n-j}, t_{n-j}) = 0,$$

$$T\Psi_n + D(C - N_n + P_n) = 0,$$

$$D \frac{1}{\tau_n} \sum_{j=0}^{k} \alpha_{j,n} N_{n-j} + j_N(A_S^\mathsf{T} e_n, \Psi_n, N_n) + R(N_n, P_n) = 0,$$

$$D \frac{1}{\tau_n} \sum_{j=0}^{k} \alpha_{j,n} P_{n-j} - j_P(A_S^\mathsf{T} e_n, \Psi_n, P_n) + R(N_n, P_n) = 0.$$

5.3 State-space matrices as a means for linking harmonic to transient analyis

We have already indicated that the MAGWEL harmonic field solver is capable of generating matrix information that can be used for transient analysis. The connection between the harmonic and transient solver approach is provided by the state-space description of the fields. As a reminder, we first summarize here the set-up of the MAGWEL solver for frequency analysis. First of all it should be noted that the MAGWEL solver in the frequency domain solves

- Solving Gauss' law.
- Solving Current-continuity equations.
- Solving Maxwell-Ampere equations,
- Respecting the gauge condition is a side product of solving above set.

These equations are solved with the following sign conventions

$$\nabla \cdot \mathbf{D} - \rho = 0 \tag{118}$$

This choice leads to discretization matrices with positive diagonal entries The current-continuity equation for conductors is solved for the same reason in the following form :

$$\nabla \cdot \mathbf{J} + \frac{\partial \rho}{\partial t} = 0 \tag{119}$$

In the frequency domain this becomes

$$\nabla \cdot \mathbf{J} + \mathrm{i}\omega\rho = 0 \tag{120}$$

since any small-signal (AC) solution is assumed to have the following appearance : $X(t) = X_0 + \mathrm{e}^{\mathrm{i}\omega t}\, X_1$

The small-signal parts of the hole- and electron current continuities are solved in the following form

$$\nabla \cdot \mathbf{J}_\mathrm{p} + \mathrm{i}q\omega p + q(r - G) = 0 \tag{121}$$

$$-\nabla \cdot \mathbf{J}_\mathrm{n} + \mathrm{i}q\omega p + q(r - G) = 0 \tag{122}$$

The choice of the sign convention is motivated by having positive diagonal matrix entries. In here, q denotes the positive unit of charge and p, n, R, G the carrier densities for holes and electrons, the recombination and the generation.

Finally, the small-signal parts of the Maxwell-Ampere equation is addressed in the following form :

$$\nabla \times \left(\frac{1}{\mu}\nabla \times \mathbf{A}\right) - \frac{1}{\mu}\nabla\left(\nabla \cdot \mathbf{A}\right) + \sigma\nabla V + \mathrm{i}\omega\sigma\ \mathbf{A} - \epsilon\omega^2\mathbf{A} = 0 \tag{123}$$

where the minus sign of the last term is the result of i^2. In the last equation we have not included the diffusive part of the carrier currents but these ones can be easily taken into account. However, their inclusion has limited validity since for non-linear materials the method that is described in this section is not usable. Thus, this section applies to insulators and inductors only. At this stage we should compare equation (123) with equation (26). Transforming the latter to the frequency domain gives

$$\epsilon(\mathrm{i}\omega)(\mathrm{i}\omega)\mathbf{A} + \nabla \times \left(\frac{1}{\mu}\nabla \times \mathbf{A}\right) - \frac{1}{\mu}\nabla\left(\nabla \cdot \mathbf{A}\right) + \sigma\nabla V + \mathrm{i}\omega\sigma\ \mathbf{A} = 0 \tag{124}$$

We now proceed with the discretization of above equations. The result will be that a linear problem is given for a set of variables

$$A(\omega)\mathbf{X} + \mathbf{b} = 0 \tag{125}$$

Here $\mathbf{X} = \{V_1, V_2, ...V_n, A_1, A_2, ...A_m\}$ in which V and A have the same meaning as before on the discretized grid. The matrix A is frequency dependent and the vector $\mathbf{b}$ describes the coupling to the contact potentials.

We now come to a key observation of the harmonic solver.

There is a one-to-one mapping of the system of equations in the time domain with the equations in the frequency domain, provided that the materials are linear.

The time-dependent system

$$\left[A_0 + A_1\frac{\mathrm{d}}{\mathrm{d}t} + A_2\frac{\mathrm{d}^2}{\mathrm{d}t^2}\right]\mathbf{X}(t) + \mathbf{b}(t) = 0 \tag{126}$$

maps with the insertion $X(t) = X_0 + \mathrm{e}^{\mathrm{i}\omega t}\, X_1$ onto

$$\left[A_0 + \mathrm{i}\omega A_1 + (\mathrm{i}\omega)^2 A_2\right]\mathbf{X} + \mathbf{b}_0 + (\mathrm{i}\omega)\mathbf{b}_1 + (\mathrm{i}\omega)^2\mathbf{b}_2 = 0 \tag{127}$$

We will now elaborate on the vector $\mathbf{b}$. For that purpose we remind us of the coupling of the field degrees of freedom to the boundary conditions. The voltage boundary conditions at the contacts, are collected in a set $\mathbf{U} = \{u_1, u_2, , , , u_{n^c}\}$. In the MNA, these variables are denoted as $\{e_1, e_2, ...\}$, however, here we follow a 'state-space convention'. The coupling is a $n \times n^c$ matrix B such that

$$\mathbf{b}(t) = B\ \mathbf{U}(t) \tag{128}$$

In order to obtain an explicit expression for the matrix B, we consider the situation that the contacts is attached to conductors and moreover, that the current-continuity equations must be solved. We use similar methods as described in detail in section 4.2.2. The assembling rule for any conductor or conductor/insulator interface node is :

$$\sum_j \sigma\left[\frac{S_{ij}}{h_{ij}}\left(V_i - V_j\right) - \sigma_{ij}\frac{\mathrm{d}A_{ij}}{\mathrm{d}t}S_{ij}\right] + \frac{\mathrm{d}}{\mathrm{d}t}\sum_j \epsilon\left[\frac{S_{ij}}{h_{ij}}\left(V_i - V_j\right) - \sigma_{ij}\frac{\mathrm{d}A_{ij}}{\mathrm{d}t}S_{ij}\right] = 0 \qquad i \subset \mathcal{N}_\infty \tag{129}$$

Here we apologize for the multiple use of the symbol σ. The one without labels stands for the conductance, whereas the one with labels keeps track of the direction of $\mathbf{A}$ with respect to the link orientation $\mathbf{n}$. Furthermore, we can divide the sums over internal nodes, i.e. degrees of freedom and contact nodes. There are no link degrees of freedom that are 'external'. For Dirichlet's boundary conditions, the links on the surface of the simulation domain have zero vector potential. As a consequence, the B matrix has an expansion in $\mathrm{d}/\mathrm{d}t$ up to first order. Therefore, equation (126) becomes

$$\left[A_0 + A_1\frac{\mathrm{d}}{\mathrm{d}t} + A_2\frac{\mathrm{d}^2}{\mathrm{d}t^2}\right]\mathbf{X}(t) + \left[B_0 + B_1\frac{\mathrm{d}}{\mathrm{d}t}\right]\mathbf{U}(t) = 0 \tag{130}$$

and as a consequence, equation (126) can be written as

$$\left[A_0 + \mathrm{i}\omega A_1 + (\mathrm{i}\omega)^2 A_2\right]\mathbf{X} + \left[B_0 + \mathrm{i}\omega\ B_1\right]\mathbf{U} = 0 \tag{131}$$

The matrices A_0, A_1, A_2, B_0, B_1 are explicitly constructed using the harmonic analysis field solver. In particular, there are also matrix elements of B that couple into the Maxwell-Ampere equation, due to the presence of the $\sigma\nabla V$ -term and the treatment of the surface nodes.

Besides the state-space variables, the observables $\mathbf{Y}$ are part of the complete model. In the present model we take the currents at the contacts as the observables of the state space. Furthermore, the currents are defined as positive (> 0), when the current is outgoing of the simulation domain. In particular, $\mathbf{Y} = \{I_1, I_2, ...I_{n^c}\}$. Thus the full picture takes the following form :

$$\begin{bmatrix} A & B \\ C & D \end{bmatrix} * \begin{bmatrix} \mathbf{X} \\ \mathbf{U} \end{bmatrix} + \begin{bmatrix} \mathbf{0} \\ \mathbf{Y} \end{bmatrix} = 0 \tag{132}$$

We will now present the detailed derivation of the matrices C and D. Our starting point will be the current-continuity equations for the contact nodes. The current continuity can be expressed as :

$$\nabla \cdot \mathbf{J} = 0 \quad \text{where} \quad \mathbf{J} = \mathbf{J}_{\text{cond}} + \mathbf{J}_{\text{disp}} \tag{133}$$

For a contact node the discrete assembling gives

$$\sum_j \Delta S_{ij} J_{ij} + I_i^{\text{out}} = 0 \tag{134}$$

In fig. (11) this is illustrated.

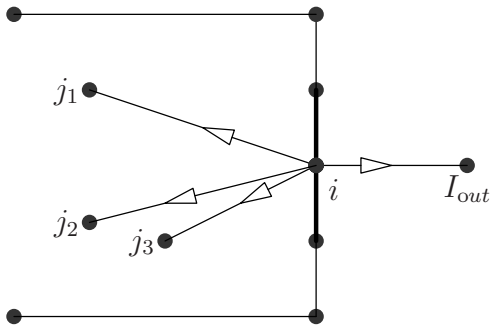

Figure 11: Illustration of the currents at a contact node, i. The nodes j are field nodes.

The total current for the contact is obtained by summing over all the contact nodes :

$$I^{\text{out}} = \sum_i I_i^{\text{out}} \tag{135}$$

The assembling of the current-continuity equations for internal nodes, j, runs over all links that are connected to j, including the contact nodes i. Whereas in the stand-alone field solving approach these contributions are not considered for the matrix building, we can evaluate these contributions for the construction of the matrices C and D. Using the fact that $J_{ij} = -J_{ji}$, the assembling leads to the following result :

$$\begin{aligned} -\sum_j \frac{\Delta S_{ij}}{h_{ij}} \sigma V_j + \sum_j \frac{\Delta S_{ij}}{h_{ij}} \sigma V_i + \sum_j \Delta S_{ij} \sigma \sigma_{ij} \frac{\mathrm{d}}{\mathrm{d}t} A_{ji} \\ -\sum_j \frac{\Delta S_{ij}}{h_{ij}} \frac{\mathrm{d}}{\mathrm{d}t} \epsilon V_j + \sum_j \frac{\Delta S_{ij}}{h_{ij}} \frac{\mathrm{d}}{\mathrm{d}t} \epsilon V_i \\ +\sum_j \Delta S_{ij} \epsilon \sigma_{ij} \frac{\mathrm{d}^2}{\mathrm{d}t^2} A_{ji} + I_i^{\text{out}} = 0 \end{aligned} \tag{136}$$

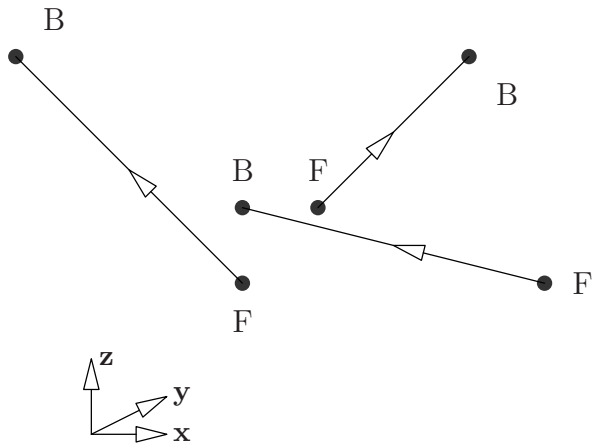

Figure 12: A collection of oriented links.

For each term we can read off their contribution to the matrices C and D. Remembering that V_i is an entry in the stimulus vector $\mathbf{U}$ and V_j is one of the entries of $\mathbf{X}$, we find that $-\sum_j \Delta S_{ij}\sigma$ contributes to the zeroth-order term C_0, i.e.

$$C = C_0 + \mathrm{i}\omega C_1 + (\mathrm{i}\omega)^2 C_2 \tag{137}$$

Furthermore $\sum_j \Delta S_{ij}\sigma$ contributes to D_0

$$D = D_0 + \mathrm{i}\omega D_1 + (\mathrm{i}\omega)^2 D_2 \tag{138}$$

5.4 A technical detail: Link orientations

The orientation of the link direction is not related to some preferred direction of the coordinate system. In figure (12) a collection of links is shown, including their orientation. As is seen the orientation of a link is just an convention of which node is used as the front node and which node is seen as the back node.

We may now take the unit vector $\hat{\mathbf{n}}$ which points from the front node to the back node and project the electric field on this vector. This gives:

$$\mathbf{E} \cdot \hat{\mathbf{n}} = -\hat{\mathbf{n}} \cdot \nabla V - \mathrm{i}\omega\, \hat{\mathbf{n}} \cdot \mathbf{A} \tag{139}$$

The variable A_{ij} is defined as:

$$A_{ij} = A_{ji} = \hat{\mathbf{n}} \cdot \mathbf{A} \tag{140}$$

The indices, ij just remind us between which nodes the link is located.

The potential term is by construction, with ΔL the length of the link:

$$\hat{\mathbf{n}} \cdot \nabla V = \frac{V_B - V_F}{\Delta L} \tag{141}$$

In order to incorporate this convention into the construction of the discretized versions of the continuity equations and Gauss' law, we start from some node i and consider the link to node j. Then there are two possibilities:

- i is the front node F and j is the back node B. Then $\sigma_{ij} = +1$
- i is the back node B and j is the front node F. Then $\sigma_{ij} = -1$
- $E_{ij} = -\frac{V_j - V_i}{h_{ij}} - \sigma_{ij}(\mathrm{i}\omega)A_{ij}$ where $h_{ij} = \Delta L$

6 'Off-shell' interpretation of the state-space equations

In a stand-alone field solver view, the variables $\mathbf{U}$ are considered as fixed in each simulation experiment. However, now we get into a situation that the excitations on the field solver are driven by branches from a circuit network. Using modified nodal analysis, the voltages that determine the branch equations are themselves variables. As a consequence, we must consider the state-space equations as 'homogeneous linear equations' for the variables $\mathbf{X}$ and $\mathbf{U}$. The view that $\mathbf{U}$ are variables contrary to fixed values can be seen as an 'off-shell' interpretation. [5]

The set up of the MNA showed that we guarantee that there are as many as unknowns (MNA-variables) as there are equations. For that purpose the KCLs and KVLs as well as the BCEs and are needed. Once that all branches are fully described the solving can be done. Now, suppose that we eliminate branches from the network. Attempting to solve the new network in general lead to a completely different solution or no solution at all if the resulting problem is not well-defined anymore. We will now discuss the relationship of the circuit modeling and the field solving. In Fig. 13 we show how the field solver couples into the MNA matrix system. For comparison, we also included an illustration of how a simple resistor is coupled into the MNA.

Comparing the simple resistor with the field solver, we observe that the role of the field solver is to provide an admittance matrix for the collection of contacts that are connected to a field-solving sector.

$$\begin{bmatrix} I_1 \\ I_2 \\ . \\ . \\ I_n \end{bmatrix} = \begin{bmatrix} Y_{11} & Y_{12} & . & . & Y_{1n} \\ Y_{21} & Y_{22} & . & . & Y_{2n} \\ . & . & . & . & . \\ . & . & . & . & . \\ Y_{n1} & Y_{n2} & . & . & Y_{nn} \end{bmatrix} * \begin{bmatrix} u_1 \\ u_2 \\ . \\ . \\ u_n \end{bmatrix} \tag{142}$$

From the example in Fig. 13, we can now learn how to set up the complete set of equations again. When the resistor is glued on on the nodes with nodal voltages e_{k1} and e_{k2} then these nodes each add one KCL equation. Furthermore one BCE is added. For the resistor, this is a $1x1$ admittance matrix. This part is replaced by the field solver. Thus the complete MNA + FS collection of variables consists of the following variables:

- $\mathbf{X}$: all internal field degrees of freedom
- $\mathbf{U}$: all contact potentials of the field solver
- $\mathbf{Y}$: all currents at the contacts of the field solver
- $\mathbf{e}$: all the voltages of the MNA including the ones to which the field solver will be attached
- $\mathbf{i}$: all branch currents including the ones to the nodes where the field solver will be attached

[5] The problem under consideration is very simulator to the evaluation of Feynman diagrams containing external legs. When these diagrams represent a direct interpretation of collision the legs are 'on-shell'. If the diagram is part of bigger diagrammatic entity the legs are 'off-shell'.

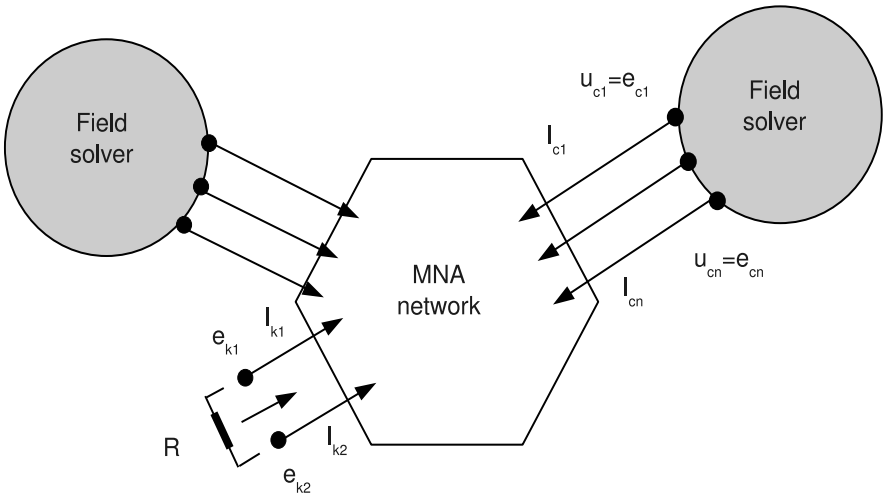

Figure 13: Illustration of the coupling off a field solver in a MNA solver.

Furthermore, the system is completed with the following constraint from the actual attachment :

- $\mathbf{U} \subset \mathbf{e}$
- $\mathbf{Y} \subset \mathbf{i}$

7 Elaborating an example

For the prototype inductor we consider the equation set up from a field-solving perspective. There are no semiconductor nodes and therefore the variables are the node potentials and the projections0 of the vector potentials on the links. For this example the following data are found: The # number of nodes = 4x6x8 = 192

parameter	value
# nodes	192
# contact nodes	8
# number of M/I nodes	40
# number of dielectric nodes	144
# number of links	472
# number of edge links	284

This leads to the following set of degrees of freedom. For the nodes we have to subtract the contact nodes.

parameter	value
# V - nodes	184
# A - links	188
# sum	372

The degrees of freedom are coupled according to the following matrix decomposition.

The matrix ”VA-MTE-MMF-1-F0-MATRIX” describes the entries of the time-independent part of the linear system. A glimps of this matrix with 2144 entries is shown below.

```
% File in matrix - market format
% number if non-zeros: 2144
%     row    col    value
372 372 2144
1 1 30584863567.102 0
1 2 -134995259.882384 0
1 5 -75934833.6838412 0
1 21 -30373933473.5358 0
2 1 -134995259.882384 0
2 2 61169727134.2041 0
2 6 -151869667.367682 0
2 22 -60747866947.0716 0
3 3 61169727134.2041 0
3 4 -134995259.882384 0
3 7 -151869667.367682 0
3 23 -60747866947.0716 0

....

....

....
371 338 -250.988826925752 0
371 365 -0.62747206731438 0
371 370 -1.11550589744779 0
371 371 254.474782855276 0
371 372 -1.11550589744779 0
372 341 -250.988826925752 0
372 366 -0.62747206731438 0
372 371 -1.11550589744779 0
372 372 254.474782855276 0
```

The matrix ”VA-MTE-MMF-1-F1-MATRIX” describes the first-order time derivatives is shown below. This matrix has 696 entries.

```
% File in matrix - market format
% number if non-zeros: 696
%     row    col    value
372 372 696
```

```
1 1 1788.07751960039 0
1 2 -3.54173122439671 0
1 5 -1.99222381372315 0
1 21 -796.889525489263 0
1 50 -978.856425010433 0
1 90 -2.44714106252608 0
1 97 -4.35047300004637 0
1 189 -1694115095.92083 0
1 204 -1270586321.94063 0
1 269 -25411726438.812 0
2 1 -3.54173122439671 0
2 2 1604.84696105477 0
2 6 -1.53730656492021 0
2 22 -614.922625968093 0
2 51 -978.856425010433 0
2 91 -2.44714106252608 0
2 189 1694115095.92083 0
2 192 -1694115095.92083 0
2 207 -2541172643.88125 0
2 272 -50823452877.6239 0

...

...

...

355 154 6.37788389003785e-05 0
356 155 6.37788389003785e-05 0
357 156 5.31490324169821e-05 0
358 157 5.31490324169821e-05 0
359 158 6.37788389003785e-05 0
360 159 6.37788389003785e-05 0
361 162 6.37788389003785e-05 0
362 163 6.37788389003785e-05 0
363 164 5.31490324169821e-05 0
364 165 5.31490324169821e-05 0
365 166 6.37788389003785e-05 0
366 167 6.37788389003785e-05 0
367 170 6.37788389003785e-05 0
368 171 6.37788389003785e-05 0
369 172 5.31490324169821e-05 0
370 173 5.31490324169821e-05 0
371 174 6.37788389003785e-05 0
372 175 6.37788389003785e-05 0
```

Finally, the matrix ”VA-MTE-MMF-1-F2-MATRIX” describes the second-order variation in time. It contains 428 non-zero elements.

```
% File in matrix - market format
% number if non-zeros: 428
%     row    col    value
372 372 428
1 185 40.9470043070174 0
1 186 54.5960057426898 0
1 187 818.940086140347 0
1 189 -44.4467482648819 0
1 204 -33.3350611986614 0
1 269 -666.701223973231 0
2 188 40.9470043070174 0
2 189 44.4467482648819 0
2 190 818.940086140347 0
2 192 -44.4467482648819 0
2 207 -25.7231180903054 0
2 272 -514.462361806115 0
3 197 40.9470043070174 0
3 198 44.4467482648819 0
3 199 818.940086140347 0
3 201 -44.4467482648819 0
3 216 -25.7231180903054 0
3 281 -514.462361806115 0

...

...

...


360 360 5.33592531943084e-05 0
361 361 5.33592531943084e-05 0
362 362 5.33592531943084e-05 0
363 363 4.44660443285904e-05 0
364 364 4.44660443285904e-05 0
365 365 5.33592531943084e-05 0
366 366 5.33592531943084e-05 0
367 367 5.33592531943084e-05 0
368 368 5.33592531943084e-05 0
369 369 4.44660443285904e-05 0
370 370 4.44660443285904e-05 0
371 371 5.33592531943084e-05 0
372 372 5.33592531943084e-05 0
```

This matrix is diagonal in the part that describes the A-A coupling. Actually this part is related to Π_{ij}.

In order to make sense of the numerical values, it should be kept in mind that all values refer to scaled quantities. The scaling is done by the following set of scaling parameters.

```
Name Value
 Density         1e+16
 Temperature     300
 Voltage         0.025852151443658
 Length(meter)   1.19527233014538e-05
 Length(micron)  11.9527233014538
 Diffusion       1
 Mobility        38.6815001521012
 Current Density 134.043092907967
 Time            1.42867594321117e-10
 Electric Field  2162.86705478354
 Frequency       6999487915.72946
 Theta Field     3.69343468478062e-12
 A field         3.09003612953325e-07
 Conductance     0.0619747259136934
 K_parameter     7.78797374554801e-08
 Velocity        83662.942308584
 Auger           6.99948791572945e-23
 Current         1.91504142191233e-08
 Volume          1.70765682366467e-15
 B field         0.025852151443658
 Surface charge  1.91504142191233e-08
 Area            1.42867594321117e-10
 Inverse Area    6999487915.72946
 Resistance      1349952.59882381
 Inductance      0.000192864480241499
 Capacitance     1.05831563601267e-16
```

Up to this point we have described the coupling of the internal degrees of freedom to each other. We will now continue with describing the coupling the the external inputs, i.e. the voltages on the contacts. Thus we provide a matrix that has size $N_{dof} \times N_{contacts}$. Since only a limited number of degrees of freedom couple to the contacts, we will present her the complete matrices explicitly. Since the number are printed as complex<double> we observe that the imaginary parts are equal to zero.

The matrix is has an Taylor expansion

$$\mathbf{B} = \mathbf{B}_0 + \mathbf{B}_1 \frac{\mathrm{d}}{\mathrm{d}t} \tag{143}$$

The matrix $\mathbf{B}_0$ is :

```
% File in matrix - market format
% number if non-zeros: 28
```

```
%         row    col      value
372     2     28
2       1       134995259.882384        0
3       2       134995259.882384        0
6       1       134995259.882384        0
7       2       134995259.882384        0
22      1       134995259.882378        0
23      2       134995259.882378        0
26      1       134995259.882379        0
27      2       134995259.882378        0
52      1       815.713687508695        0
53      2       815.713687508695        0
60      1       815.713687508695        0
61      2       815.713687508695        0
92      1       2.03928421877174        0
93      2       2.03928421877174        0
116     1       2.03928421877174        0
117     2       2.03928421877174        0
148     1       815.713687508694        0
149     2       815.713687508694        0
156     1       815.713687508694        0
157     2       815.713687508694        0
192     1       131.93723888968         0
198     2       -131.93723888968        0
211     1       131.93723888968         0
217     2       -131.93723888968        0
274     1       131.937238889674        0
280     2       -131.937238889674       0
293     1       131.937238889674        0
299     2       -131.937238889674       0
```

and the matrix $\mathbf{B}_1$ is :

```
% File in matrix - market format
% number if non-zeros: 36
%         row    col      value
372     2     36
2       1       3.54173122439671        0
3       2       3.54173122439671        0
6       1       3.54173122439671        0
7       2       3.54173122439671        0
11      1       2.03928421877174        0
12      2       2.03928421877174        0
22      1       3.54173122439674        0
23      2       3.54173122439674        0
26      1       3.54173122439674        0
27      2       3.54173122439674        0
```

```
31      1       2.03928421877174        0
32      2       2.03928421877174        0
```

This result says that the MA degrees of freedom (the vector potentials on the links) do not couple with time derivatives to the contact voltages. This can be understood as follows: The MA equations are link-wise discretized. Consequently each line in the MA equation system corresponds to one link. The begin- and end point voltages play a role in the link equation. The conduction current provides an entry in the B0 matrix. However, the displacement current is absorbed by the gauge condition and therefore only the nodes on the edge can still contribute to B1. These nodes must also be contacts, and since the contacts are internal, no such contribution exists for this example : B1 consists of nodal entries only.

Next we must extract from the set of degrees of freedom the output.

This information is contained in a matrix of size $N_{contacts} \times N_{dof}$.

$$\mathbf{C} = \mathbf{C}_0 + \mathbf{C}_1 \frac{\mathrm{d}}{\mathrm{d}t} + \mathbf{C}_2 \frac{\mathrm{d}^2}{\mathrm{d}t^2} \tag{144}$$

The matrix $\mathbf{C}_0$ is given as :

```
% File in matrix - market format
% number if non-zeros: 8
%         row    col      value
2       372       8
1       2       134995259.882384        0
1       6       134995259.882384        0
1       22      134995259.882378        0
1       26      134995259.882379        0
2       3       134995259.882384        0
2       7       134995259.882384        0
2       23      134995259.882378        0
2       27      134995259.882378        0
```

and the matrix $\mathbf{C}_1$ is :

```
% File in matrix - market format
% number if non-zeros: 32
%         row    col      value
2       372       32
1       2       3.54173122439671        0
1       6       3.54173122439671        0
1       11      2.03928421877174        0
1       22      3.54173122439674        0
1       26      3.54173122439674        0
1       31      2.03928421877174        0
```

```
1       52      815.713687508695        0
1       60      815.713687508695        0
1       92      2.03928421877174        0
1       116     2.03928421877174        0
1       148     815.713687508694        0
1       156     815.713687508694        0
1       192     -1694115095.92083       0
1       211     -1694115095.92083       0
1       274     -1694115095.92076       0
1       293     -1694115095.92076       0
2       3       3.54173122439671        0
2       7       3.54173122439671        0
2       12      2.03928421877174        0
2       23      3.54173122439674        0
2       27      3.54173122439674        0
2       32      2.03928421877174        0
2       53      815.713687508695        0
2       61      815.713687508695        0
2       93      2.03928421877174        0
2       117     2.03928421877174        0
2       149     815.713687508694        0
2       157     815.713687508694        0
2       198     1694115095.92083        0
2       217     1694115095.92083        0
2       280     1694115095.92076        0
2       299     1694115095.92076        0
```

Finally, the matrix $\mathbf{C}_2$ is given by

```
% File in matrix - market format
% number if non-zeros: 24
%         row    col      value
2       372       24
1       191     -34.1225035891811       0
1       192     -44.4467482648819       0
1       193     -682.450071783622       0
1       211     -44.4467482648819       0
1       212     -682.450071783622       0
1       229     34.1225035891811        0
1       273     -34.1225035891811       0
1       274     -44.4467482648823       0
1       293     -44.4467482648823       0
1       311     34.1225035891811        0
1       351     682.450071783622        0
1       357     682.450071783622        0
2       194     -682.450071783622       0
2       195     -34.1225035891811       0
```

```
2       198     44.4467482648819        0
2       213     -682.450071783622       0
2       217     44.4467482648819        0
2       233     34.1225035891811        0
2       277     -34.1225035891811       0
2       280     44.4467482648823        0
2       299     44.4467482648823        0
2       315     34.1225035891811        0
2       352     682.450071783622        0
2       358     682.450071783622        0
```

Besides the internal degrees of freedom there is also a direct mapping of the input to the output. Remembering the modified state-space discretization that also contains a $\mathbf{D}$ matrix, we also have here such a matrix that is required to specify completely the output signal in terms of the state-space variables $\mathbf{X}$ and the contact potentials $\mathbf{U}$.

$$\begin{bmatrix} \mathbf{A} & \mathbf{B} \\ \mathbf{C} & \mathbf{D} \end{bmatrix} \cdot \begin{bmatrix} \mathbf{X} \\ \mathbf{U} \end{bmatrix} + \begin{bmatrix} \mathbf{0} \\ \mathbf{Y} \end{bmatrix} = 0 \tag{145}$$

The $\mathbf{D}$ - matrix takes the following form

$$\mathbf{D} = \mathbf{D}_0 + \mathbf{D}_1 \frac{\mathrm{d}}{\mathrm{d}t} \tag{146}$$

The matrix $\mathbf{D}_0$ is :

```
% File in matrix - market format
% number if non-zeros: 2
%         row     col       value
2       2       2
1       1       -539981039.529526       0
2       2       -539981039.529526       0
```

and the matrix $\mathbf{D}_1$ is :

```
% File in matrix - market format
% number if non-zeros: 2
%         row     col       value
2       2       2
1       1       -3284.06330591  0
2       2       -3284.06330591  0
```

Note that these matrices are of 2x2 size.

WARNING: Note that all equations are assembled according to the rule $F(X) = 0$ or right-hand side is put equal zero. This is important for assigning the appropriate signs to the variables.

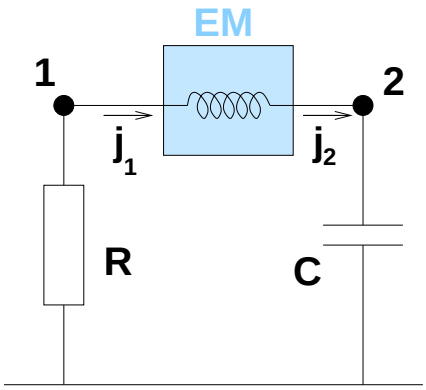

Figure 14: Simple circuit with a coil described by EM equations

7.1 The external circuit

We consider a simple circuit given in Figure 14. The coil is described by the electromagnetic system (145).

The circuit equations look in modified nodal analysis (MNA) form as

$$\mathbf{E}e + \mathbf{F}j = 0 \tag{147}$$

with

$$\mathbf{E} = \begin{pmatrix} \frac{1}{R} & 0 \\ 0 & C\frac{\mathrm{d}}{\mathrm{d}t} \end{pmatrix} \qquad \text{and} \qquad \mathbf{F} = \begin{pmatrix} -1 \\ 1 \end{pmatrix}.$$

with $j = j_1 = j_2$. Note that the incoming current j_1 of the coil has to be equal to the outflowing current j_2 of the coil for consistency reasons.

7.2 The coupled system

The coupling equations between the EM system (145) and the circuit system (147) are given by

$$\mathbf{U} = e \tag{148}$$

for the potentials and

$$\mathbf{Y} = j \tag{149}$$

for the current. For consistency reasons, we should have $j_1 = j_2$, i.e. $\mathbf{Y_1} = \mathbf{Y_2}$. This guaranteed by the EM equations. We also need to check the signs for $\mathbf{Y}$.

Note, in general, we have a larger number of node potentials e than the number of contact potentials **U**. That means, we would get an equation of the type

$$\mathbf{U} = \mathbf{K}e$$

with **K** being a full row rank rectangular matrix. Correspondingly, we would have an equation of the form

$$\mathbf{Y} = \mathbf{L}j.$$

If we plug in the coupling equations (148) and (149) into the EM system (145) and the circuit system (147) then we obtain the coupled system

$$\begin{pmatrix} \mathbf{A} & \mathbf{B} & 0 \\ \mathbf{C} & \mathbf{D} & I \\ 0 & \mathbf{E} & \mathbf{F} \end{pmatrix} \begin{pmatrix} \mathbf{X} \\ e \\ j \end{pmatrix} = 0 \tag{150}$$

with I being the identity matrix. In general, it would look like

$$\begin{pmatrix} \mathbf{A} & \mathbf{BK} & 0 \\ \mathbf{C} & \mathbf{DK} & \mathbf{L} \\ 0 & \mathbf{E} & \mathbf{F} \end{pmatrix} \begin{pmatrix} \mathbf{X} \\ e \\ j \end{pmatrix} = r(t)$$

with $r(t)$ describing independent source functions.

7.2.1 Numerical values

When simulating the ring using the field solver as a two port device, where the ground contact is used as a reference, then we obtain the following values :

Parameter	real part	imaginary part
S11	-0.121720192779	-0.323790061496
S21	0.877725879634	-0.327819765463
S12	0.877725879634	-0.327819765463
S22	-0.121720192779	-0.323790061496

These S parameters give with a 50 Ohm reference :

$$R = 2.725647459982 \;\; 10^{-02} \;\; \Omega$$
$$L = 3.206145380487 \;\; 10^{-11} \;\; \mathrm{H}$$

We can also drive the system as a 1-port. Then the following results are obtained :

Parameter	real part	imaginary part
S11	-0.998992961741	0.00603515190758
Y11	1.05597648657	-6.44829676341
Z11	0.0247326669262	0.151029476621

Since $R = Re(Z)$ and $L = Im(Z)/(2\pi f)$, we obtain

$$R = 0.0247326669262 \;\; \Omega$$
$$L = 2.40377966928 \;\; 10^{-11} \;\; \mathrm{H}$$

We can investigate the resonance of the simple circuit by taking a capacitance value that corresponds to the situation that the imaginary part of the complete circuit is equal to zero. The total impedance is

$$Z_{\text{total}} = R_{\text{ex}} + R_{\text{ex}} + \mathrm{i}\omega L + \frac{1}{\mathrm{i}\omega C} \tag{151}$$

Then resonance occurs if $\omega^2 LC = 1$ For 1GHz and $L\ 3e-11\ \mathrm{H}$ a proper choice for C is given by :

$$C = \frac{1}{\omega^2 L} = 1.05383161404\ \ 10^{-9}\ \ \mathrm{F} \simeq 1\ \ \mathrm{nF} \tag{152}$$

In order to see some effect of the resistance it makes sense to choose $R = 0.2\ \ \Omega$

8 Appendix : Scaling

In this appendix, we will have a closer look at scaling and unscaling of the field equations. For that purpose we will start from equations (154) -(156) The Maxwell are:

- *for insulators:*

$$-\nabla \cdot \left[\varepsilon \left(\nabla V + \frac{\partial \mathbf{A}}{\partial t}\right)\right] = 0 \tag{153}$$

$$\nabla \times \frac{1}{\mu}\left(\nabla \times \mathbf{A}\right) = -\varepsilon \frac{\partial}{\partial t}\left(\nabla V + \frac{\partial \mathbf{A}}{\partial t}\right) \tag{154}$$

- *for conductors:*

$$-\nabla \cdot \sigma \left(\nabla V + \frac{\partial \mathbf{A}}{\partial t}\right) = \frac{\partial}{\partial t}\left(\nabla \cdot \varepsilon \left(\nabla V + \frac{\partial \mathbf{A}}{\partial t}\right)\right) \tag{155}$$

$$\nabla \times \frac{1}{\mu}\left(\nabla \times \mathbf{A}\right) = -\sigma \left(\nabla V + \frac{\partial \mathbf{A}}{\partial t}\right) - \varepsilon \frac{\partial}{\partial t}\left(\nabla V + \frac{\partial \mathbf{A}}{\partial t}\right) \tag{156}$$

8.1 Poisson

Starting from Gauss' law, the actual expression that is programmed is:

$$\int_{\partial(\Delta v)} \mathbf{dS} \cdot (-\epsilon)\left(\nabla V + \frac{\partial \mathbf{A}}{\partial t}\right) - Q(\Delta v) = 0 \tag{157}$$

Let λ be the scaling of the length. The scaling constant has dimension [Length] = meter. Since the surface integral introduces a scaling factor λ^2, and the gradient a factor λ^{-1}. The voltage is scaled using $\sigma_V = 0.025852151443658\ [V]$. Moreover, since the vacuum permittivity is absorbed in the scaling process, the first term is :

$$\lambda \epsilon_0 \sigma_V \int_{\partial(\Delta \tilde{v})} \mathrm{d}\tilde{S} \cdot (-\epsilon_r)\tilde{\nabla}\tilde{V}$$

in which all tildes indicate scaled variables. The corresponding term that is assembled in the program is :

$$\int_{\partial(\Delta \tilde{v})} \mathrm{d}\tilde{S} \cdot (-\epsilon_r)\tilde{\nabla}\tilde{V}$$

The matrix element of the scaled equations are computed in the MAGWEL software. These matrix elements can be viewed as the proportionality factor of the contributions originating from voltage degrees of freedom. Therefore, the scaling factor of these matrix elements do not contain σ_V, and the proper way to unscale these element is by multiplying them with $\lambda\epsilon_0$. The permittivity of vacuum is in units $\epsilon_0 = 8.85418 \times 0^{-12}\ [C^2/Nm^2]$ and the length-scaling parameter is $\lambda = 1.19527233014538e-05[m]$. Therefore, $\lambda\epsilon_0 = 1.05832 \times 10^{-16}[C^2/Nm]$. In the example, we find the following values for the scaled and unscaled variables (starting at row 41) for the matrix VA-MTE-MMF-1-F0-MATRIX:

row	col	scaled	unscaled
41	41	246.413509768251	2.607832703125e-14
41	42	-1.08761825001158	-1.15104339999999e-16
41	49	-0.611785265631516	-6.47461912499996e-17
41	89	-244.714106252608	-2.58984765e-14
42	41	-1.08761825001158	-1.15104339999999e-16
42	42	492.827019536503	5.21566540625e-14
42	43	-1.08761825001158	-1.15104339999999e-16
42	50	-1.22357053126303	-1.29492382499999e-16
42	90	-489.428212505217	-5.1796953e-14
.	.	.	.

Example: scaled and unscaled matrix elements from the Poisson equation.

For the matrix elements describing the coupling to the vector potential, we consider the term

$$\int_{\partial(\Delta v)} \mathbf{dS} \cdot (-\epsilon) \left(\frac{\partial \mathbf{A}}{\partial t} \right)$$

Following the same reasoning as above, we get scale this term as:

$$\epsilon_0 \lambda^2 \sigma_A / \sigma_t \int_{\partial(\Delta \tilde{v})} \mathrm{d}\tilde{S} \cdot (-\epsilon_r) \left(\frac{\partial \tilde{\mathbf{A}}}{\partial \tilde{t}} \right)$$

Since $\sigma_t = \sigma_\omega^{-1} = 1.42867594321117 \times 10^{-10}$ [sec] and since in the expansions of the matrices, the frequency (or time differentiations) is made explicit, we do not have to incorporate this scaling factor in the transition in going from scaled to unscaled matrices, provided that we also use unscaled times. The scaling factor σ_A is also excluded, provided that unscaled vector potentials are used. Therefore, the scaling factor for the A-coupling is $\epsilon_0 \lambda^2 = 1.26498 \times 10^{-21} [\mathrm{C}^2/\mathrm{N}]$.

In the example, we find the following values for the scaled and unscaled variables (starting at row 50 and column ¿ 184) for the matrix VA-MTE-MMF-1-F1-MATRIX:

row	col	scaled	unscaled
50	187	-818.940086140347	-1.03593906e-18
51	190	-818.940086140347	-1.03593906e-18
52	193	-682.450071783622	-8.6328255e-19
53	194	-682.450071783622	-8.6328255e-19
54	199	-818.940086140347	-1.03593906e-18
55	202	-818.940086140347	-1.03593906e-18
.	.	.	.

Example: scaled and unscaled matrix elements from the Poisson equation.

8.2 Current continuity

For the current-continuity equation, the expression that is programmed is:

$$\int_{\partial(\Delta v)} \mathbf{dS} \cdot (-\sigma) \left(\nabla V + \frac{\partial \mathbf{A}}{\partial t} \right) - \frac{\partial Q(\Delta v)}{\partial t} = 0 \tag{158}$$

The same reasoning as above applies, keep in mind that we now use the conductance scaling $\sigma_c = 0.0619747259136934$ [S/m]. The V term leads to a scaling factor $\sigma_c\lambda = 7.40767 \times 10^{-07}$ [S].

In the example, we find the following values for the scaled and unscaled variables (starting at row 1) for the matrix VA-MTE-MMF-1-F0-MATRIX:

row	col	scaled	unscaled
1	1	30584863567.102	22656.25
1	2	-134995259.882384	-100.000000000002
1	5	-75934833.6838412	-56.2500000000012
1	21	-30373933473.5358	-22500
2	1	-134995259.882384	-100.000000000002
2	2	61169727134.2041	45312.5
2	6	-151869667.367682	-112.500000000002
2	22	-60747866947.0716	-45000
.	.	.	.

Example: scaled and unscaled matrix elements from the current-continuity equation.

For the A-coupling we use the scaling factor: $\sigma_c\lambda^2 = 8.85418 \times 10^{-12}[Sm]$. An example is found in the the matrix VA-MTE-MMF-1-F1-MATRIX:

8.3 Maxwell-Ampere

Finally, the Maxwell-Ampere equation is programmed starting from:

$$\begin{aligned} \frac{L}{\mu_0}\int_{\Delta S} \mathrm{d}\mathbf{S}\cdot\nabla\times\left(\frac{1}{\mu_r}\nabla\times\mathbf{A}\right) \;+\; \epsilon L\,\frac{\partial}{\partial t}\int_{\Delta S}\mathrm{d}\mathbf{S}\cdot\mathbf{\Pi} - L\int_{\Delta S}\mathrm{d}\mathbf{S}\cdot\frac{1}{\mu}\nabla\left(\nabla\cdot\mathbf{A}\right) \\ +L\int_{\Delta S}\mathrm{d}\mathbf{S}\cdot\sigma\nabla V \;+\; L\int_{\Delta S}\mathrm{d}\mathbf{S}\cdot\sigma\mathbf{\Pi} \;=\; 0 \end{aligned} \tag{159}$$

In order to decide on the appearance of the unscaled equation, we will work our way to the equivalent of the Maxwell-Ampere equation in the following form :

$$\oint \mathbf{H}\cdot\mathrm{d}\mathbf{l} = \int \mathrm{d}\mathbf{S}\cdot\left(\mathbf{J}_c + \frac{\partial\mathbf{D}}{\partial t}\right) \tag{160}$$

However, this is almost correct. The precise form is:

$$L\oint \mathbf{H}\cdot\mathrm{d}\mathbf{l} = L\int \mathrm{d}\mathbf{S}\cdot\left(\mathbf{J}_c + \frac{\partial\mathbf{D}}{\partial t}\right) \tag{161}$$

The right-hand side can be further elaborated :

$$L\oint \mathbf{H}\cdot\mathrm{d}\mathbf{l} = \int \mathrm{d}\mathbf{S}\cdot\nabla\times\mathbf{H} = L\,\frac{1}{\mu_0}\int \mathrm{d}\mathbf{S}\cdot\nabla\times\frac{1}{\mu_r}\mathbf{B} = \frac{L}{\mu_0}\int \mathrm{d}\mathbf{S}\cdot\nabla\times\left(\frac{1}{\mu_r}\nabla\times\mathbf{A}\right)$$

As a consequence, the scaling factor for the second term in (159) is : $\lambda/\mu_0 = 9.51167$ [$\mathrm{m^2kg/C^2}$].

Finally, the coupling of the voltage V into the unscaled MA equation is : $\sigma_c\lambda^2 = 8.85418 \times 10^{-12}$[Sm]. This completes our scaling considerations.

9 Conclusions

This document describes the mathematical details and subtleties in order to successfully perform transient and coupled circuit-field solver approaches. The key concern is to end up after discretization with a non-singular problem such that the linear solvers are confronted with a well-defined problem. Moreover, the discretization should respect basic physical requirement such as for example charge conservation. Our discretization scheme respects these requirements. Having a well-defined problem from the (mathematical perspective) provides an answer in a finite run time, but not necessarily the $correct$ answer. For that purpose it is needed that a sufficient amount of structural detail is included. In practice it requires that the the computational mesh is fine enough to capture the relevant details. In deliverable D3.1 , we have already illustrated the need for spatial adaptive meshing, as well as the availability in the tools. In deliverable D3.3 , the temporal adaptive work will be described.

References

[1] Codestar website. http://www.imec.be/codestar/.

[2] Cmos backbone for 2010 e-europe, nanocmos, from the 45nm node down to the limits. IST-Proposal, 2003.

[3] G. Alì, A. Bartel, M. Günther, and C. Tischendorf. Elliptic partial differential-algebraic multiphysics models in electrical network design. *Math. Models Meth. Appl. Sci.*, 13(9):1261 – 1278, 2003.

[4] Richard Barrett, Michael Berry, Tony F. Chan, James Demmel, June M. Donato, Jack Dongarra, Victor Eijkhout, Roldan Pozo, Charles Romine, and Henk Van der Vorst. *Templates for the Solution of Linear Systems: Building Blocks for Iterative Methods*. SIAM, 1994. http://www.netlib.org/templates/Templates.html.

[5] M. Bodestedt and C. Tischendorf. PDAE models of integrated circuits and index analysis. *Math. Comput. Model. Dyn. Syst.*, 13(1):1–17, 2007.

[6] M. Clemens, S. Drobny, H. Kruger, P. Pinder, O. Podebrad, B. Schillinger, B. Trapp, T. Weiland, M. Wilke, M. Bartsch, U. Becker, and M. Zhang. The electromagnetic simulation software package mafia 4. In *Computational Electromagnetics and Its Applications, 1999. Proceedings.*, pages 565–568, 1999.

[7] Bart Denecker. *De subdomein FDTD methode*. PhD thesis, Universiteit Gent, 2003.

[8] D. Estévez Schwarz and C. Tischendorf. Structural analysis of electric circuits and consequences for MNA. *Int. J. Circ. Theor. Appl.*, 28:131–162, 2000.

[9] I. Higueras, R. März, and C. Tischendorf. Stability preserving integeration of index-1 DAEs. *APNUM*, 45:175–200, 2003.

[10] I. Higueras, R. März, and C. Tischendorf. Stability preserving integeration of index-2 DAEs. *APNUM*, 45:201–229, 2003.

[11] Snezana Jenei. *Characterization and optimization of the RF performances of analog components in CMOS and BiCMOS*. PhD thesis, KUL-IMEC, 2003.

[12] Domenico Lahaye. *Algebraic multigrid for two-dimensional time-harmonic magnetic field computations*. PhD thesis, KUL, 2001.

[13] S.E. Laux. Techniques for small-signal analysis of semiconductor devices. *IEEE Trans. Computer-Aided Design*, 4(10):472–481, 1985.

[14] Wil Schilders and Jan Ter Maten (Eds). *Handbook of Numerical Analysis : Numerical Methods in Electromagnetism*. Elsevier Publishing Company, the Netherlands, 2003.

[15] Wim Schoenmaker, Wim Magnus, and Peter Meuris. Strategy for electromagnetic interconnect modeling. *IEEE Trans. on CAD*, 20:753–762, 2001.

[16] Wim Schoenmaker, Wim Magnus, and Peter Meuris. Ghost fields in classical gauge theories. *Phys. Rev. Lett*, 88(18):181602–1 – 181602–4, 2002.

[17] Wim Schoenmaker, Wim Magnus, Peter Meuris, and Bert Maleszka. Renormalization group meshes and the discretization of tcad equations. *IEEE Trans. on CAD*, 21(12):1425–1433, 2002.

[18] Wim Schoenmaker and Peter Meuris. Electromagnetic interconnects and passives modeling: Software implementation issues. *IEEE Trans. on CAD*, 21:534–543, 2002.

[19] Sebastian Schöps. Coupling and simulation of lumped electric circuits refined by 3-D magnetoquasistatic conductor models using MNA and FIT. Master's thesis, Bergische Universität Wuppertal, 2008.

[20] Monica Selva Soto and Caren Tischendorf. Numerical analysis of DAEs from coupled circuit and semiconductor simulation. *Appl. Numer. Math.*, 53(2-4):471–488, 2005.

[21] A. Sidi. Efficient implementation of minimal polynomial and reduced rank extrapolation methods. *J. Comput. Appl. Math.*, 36:305–337, 1991.

[22] J. Stoer and R. Bulirsch. *Introduction to Numerical Analysis, 2nd ed.* New York: Springer-Verlag, 1993.

[23] Caren Tischendorf. *Coupled Systems of Differential Algebraic and Partial Differential Equations in Circuit and Device Simulation. Modeling and Numerical Analysis*. 2004. Habilitation thesis at Humboldt Univ. of Berlin.

[24] K. Yee. Numerical solution of initial boundary value problems involving maxwell's equation in isotropic media. *IEEE Trans. on Antennas and Propagation*, AP-14:302–307, 1966.